Research Article GU J Sci 37(4): x-x (2024) DOI: 10.35378/gujs.1422427

Gazi University

Journal of Science

http://dergipark.gov.tr/gujs

Fabricating of Turquoise/White Luminescent Azo-Schiff Bases Bearing Benzimidazole and Imidazole Rings

Ozlem GUNGOR[1,*]

Gazi University, Faculty of Science, Department of Chemistry, 06500, Ankara, Türkiye

Highlights

- This research focuses on the designing of new azo-dyes and heteroaromatic bis-Schiff bases.
- Solvato-, acido- and thermo-chromism properties have been investigated in different solvents.
- Strong white and turquoise luminescence have been observed in solution for azo-Schiff bases.

Article Info

Received: 19 Jan 2024
Accepted: 03 Jul 2024

Keywords

Azo-Schiff bases
Benzimidazole
Imidazole
Turquoise luminescence
White luminescence

Abstract

New azo dyes (**1a-b**) were produced by the azo coupling of 2-nitro-1,4-phenylenediamine with 5-chlorosalicylaldehyde and 5-chloro-2-hydroxyaniline. Corresponding Schiff base derivatives (**2a-b**) bearing conjugated benzimidazole and imidazole moieties were obtained via the condensation reaction of these dyes with 2-aminobenzimidazole and 4-imidazolecarboxaldehyde. Their structures were identified by IR, $^{1}H/^{13}C$ NMR, mass and UV–Vis spectroscopies and microanalysis. Chromic (solvato-, acido-, thermo-) and photoluminescence behaviour of compounds **2a** and **2b** were evaluated depending on their donor–π–acceptor molecular system and intramolecular proton tautomerism. Electronic absorption and photoluminescence spectra of **2a** and **2b** were recorded in DMSO, DMF and $CHCl_3$. **2a** emitted turquoise luminescence in DMSO and DMF, and white luminescence in $CHCl_3$, while **2b** emitted strong turquoise luminescence in only $CHCl_3$.

1. INTRODUCTION

Intramolecular proton transfer process occurs between tautomeric forms of a molecule in a six-membered chelate ring via hydrogen bonding interaction in ground (IPT) and excited states (ESIPT) [1]. IPT and ESIPT process generates thermochromism and photochromism, respectively. Chromism is defined as the reversible change in color due to the change in the optical properties (transmittance, reflection and absorption) of the molecule by a method caused by a physical (humidity, pressure, temperature, light, electric field, magnetic field, etc.) or chemical (pH, solution, etc.) stimulus [2]. If the changing color of the molecule between two chemical structure to give a distinguishable absorption spectrum occurs with the effect of light, temperature, solution or pH change, it is named photochromism, thermochromism, solvatochromism and halochromism, respectively. Chromic organic colorants are used in the production of smart textile materials to utilize in the fields of medicine, health and safety [3,4]. Electrochromic, thermochromic and photochromic materials have applications in many fields such as tiles, glasses, windows and optics. Halochromic and photochromic materials have great potential for optical devices and biosensor applications [5].

Azo dyes are the class of dye group used in the textile and dye industry due to their easy synthesis, high dyeing efficiency and good thermal stability [6]. These azo dyes have functional applications such as photodynamic therapy and laser dyes, related to their photoelectric properties [7–9]. Schiff bases (imine, azomethine) and metal complexes exhibit a broad spectrum of antimicrobial, antifungal, antitumor, antioxidant, enzyme inhibition activities [10,11]. These compounds demonstrate a wide range of working areas as dye, polymer stabilizer, catalyst, corrosion inhibitor and chemosensors [12]. They are used in light-

*e-mail: ozlemgungor@gazi.edu.tr

emitting electrochemical cells (LEECs), conductors and semiconductors, due to linear, non-linear optical and photochromic properties [13,14].

With this perspective, azo-linked Schiff bases are promising to have chromic and optical properties close or superior to these two organic molecule classes. To date, several papers have been reported on azo-Schiff bases bearing various heteroaromatic rings like as pyrazole [15], 1H-pyrazol-3(2H)-one [16], oxazole [17], oxadiazole [18], 9-ethylcarbazole [19], imidazole [20, 21], triazole [22], indole [23], pyridine [24], pyrimidine [25], chromone [26] and nicotinic acid [27]. Advantages of azo heterocycles is their fastness, brightness and extraordinary colouring properties [28,29]. These azo compounds have applications as chemosensing, optical switching, optical data storage and organic sensitized solar cells [30–32]. Benzimidazole and imidazole are important pharmacophores in medicinal chemistry [33,34]. They have been used as ionic liquid, optical and electronic materials, depending on their interesting characteristic photophysical properties [35,36]. Their derivatives are extensively applied as chemosensors for the sensing of metal cations and inorganic ions [37].

Here, heteroaromatic azo-Schiff bases (**2a-b**) based on benzimidazole and imidazole have been reported for the first time. For this purpose, azo dyes (**1a-b**) were obtained by the coupling reaction of 2-nitro-1,4-phenylenediamine with 5-chlorosalicylaldehyde and 5-chloro-2-hydroxyaniline. Later, these dyes were condensed with 2-aminobenzimidazole and 4-imidazolecarboxaldehyde to form azo-Schiff bases in high yield. They were identified by different spectral techniques. Imine derivatives (**2a-b**) have assessed for solvatochromic, acidochromic, thermochromic and photoluminescence properties depending on the formation of azo-imine ↔ azo-amine and azo-imine ↔ hydrazone-imine tautomeric equilibria.

2. MATERIAL METHOD

All chemicals and solvents were reagent grade. Melting points were recorded by using open capillaries on a Stuart SMP30 and were uncorrected. Microanalysis was measured on a Elemental Analyzer (Thermo Scientific Flash 2000). Infrared spectra were carried out using ATR spectrometer (Thermo Scientific Nicolet iD5). ^{1}H NMR and ^{13}C NMR spectra were recorded in DMSO-d_6 on a Varian Mercury spectrometer (Agilent, 400 MHz/100 MHz). NMR signals were abbreviated as follow, s: singlet, d: doublet, m: multiplet. Mass spectra were recorded on a mass spectrometer (Agilent LC Q-TOF) by using (ESI+) electron ionization method. Electronic absorption spectra were carried out on a spectrophotometer (Analytik Jena Specord 200). Photoluminescence spectra were carried out using HORIBA Jobin Yvon spectrometer. Absorption and emission spectra were recorded in dimethyl sulfoxide (DMSO), *N*,*N*-dimethylformamide (DMF) and chloroform ($CHCl_3$) (C = 30 μM).

2.1. Synthesis of Azo Dyes (1a-b)

The synthesis process was carried out according to the literature [38]. 2-nitro-1,4-phenylenediamine (1.0 equiv) was dissolved in cold water containing HCl (4 mL). Sodium nitrite solution (10.0 equivalent) in cold water was added to a stirred amine solution in an ice bath (0–5 ºC) drop by drop for 30 min. On the other hand, a coupling agent (aldehyde or amine) (2.0 equiv) was dissolved in aqueous ethyl alcohol solution containing sodium hydroxide (25.0 equiv). Thereafter, basic aldehyde/amine solution was added to freshly prepared diazonium solution for 30 min at 0–5 ºC. The obtained mixture was firstly stirred at 0–5 ºC for 3 h, and then stirred at room temperature for 2 days. For **1b**, pH of the resultant mixture was adjusted to 7 by using dilute aqueous NaOH solution. The obtained product was filtered, washed with water and ethyl alcohol and dried at room temperature.

3,3'-((2-nitro-1,4-phenylene)bis(diazene-2,1-diyl))bis(5-chloro-2-hydroxybenzaldeyde) (1a). The product was obtained by using an aldehyde (5-chlorosalicylaldehyde). Dark brown powder; 63%; dp 137 ºC (decomposition point). IR ν (cm^{-1}): 3217 (O–H), 3076 (Ar–H), 2876 (C–H), 1679/1656 (C=O), 1613 (C=C), 1529 (N=N), 1469 (NO_2 asym), 1345 (NO_2 sym), 1262 (C–O). ^{1}H NMR δ (ppm): 7.51–7.59 (t-d, J = 2.78 Hz, J = 2.72 Hz, 2H, Ar-H), 7.72 (s, 1H, Ar–H), 7.80 (s, 1H, Ar–H), 7.93 (s, 1H, Ar–H), 8.15 (s, 1H, Ar–H), 8.25 (s, 1H, Ar–H), 10.06 (s, 2H, OH), 10.21 (s, 2H, CHO). ^{13}C NMR δ (ppm): 119.60, 122,73, 123.73, 125.56, 127.44, 135.81, 136.56, 137.64, 144.17, 149.96, 157.82 (Ar–C), 159.39 (C–OH), 189.83 (CHO).

UV–Vis (DMSO, 30 µM): λ_{max} (nm): 396 (logε = 4.30). Anal. calcd. for ($C_{20}H_{11}Cl_2N_5O_6$) (488.24 g/mol): C, 49.20%; H, 2.27%; N, 14.34%. Found: C, 49.55%; H, 2.39%; N, 14.93%. MS (ESI+): *m/z* = 452.5663 $[(M - Cl)]^+$, calcd. 453.0467 $[(M - Cl)]^+$.

6,6'-((2-nitro-1,4-phenylene)bis(diazene-2,1-diyl))bis(2-amino-4-chlorophenol) (1b). The product was obtained by using an amine (5-chloro-2-hydroxyaniline). Dark brown powder; 76%; dp 125 ºC. IR *ν* (cm^{-1}): 3452 (O–H), 3346/3184 (NH_2), 3087 (Ar–H), 2840 (C–H), 1624 (C=C), 1563 (N=N), 1509 (NO_2 asym), 1339 (NO_2 sym), 1246 (C–O). ^{1}H NMR *δ* (ppm): 6.34 (s, 4H, NH_2), 7.24 (s, 2H, Ar–H), 7.45 (s, 2H, Ar–H), 7.67 (s, 1H, Ar–H), 7.91 (s, 1H, Ar–H), 8.38 (s, 1H, Ar–H), 10.09 (s, 2H, OH). ^{13}C NMR *δ* (ppm): 115.63, 117.80, 119.67, 125.94, 128.41, 129.98, 134.98, 135.88, 140.89, 148.07, 149.25 (Ar–C), 153.00 (C–OH). UV–Vis (DMSO, 30 µM): λ_{max} (nm): 402 (logε = 4.40). Anal. calcd. for ($C_{18}H_{13}Cl_2N_7O_4$) (462.25 g/mol): C, 46.77%; H, 2.83%; N, 21.21%. Found: C, 47.05%; H, 2.19%; N, 20.93%. MS (ESI+): *m/z* = 425.3163 $[(M - Cl)]^+$, calcd. 427.0796 $[(M - Cl)]^+$.

2.2. Synthesis of Azo-Schiff Bases (2a-b)

Azo dye (**1a-b**) (1.0 equiv) was dissolved in ethyl alcohol. This solution was mixed with coupling agent (aldehyde or amine) (2.0 equiv) by refluxing for 5 h. The final mixture was stand at ambient temperature for 3 days. The obtained product was filtered and recrystallized with ethyl alcohol.

6,6'-((2-nitro-1,4-phenylene)bis(diazene-2,1-diyl))bis(2-(((1H-benzo[d]imidazol-2-yl)imino)methyl)-4-chlorophenol) (2a). The product was obtained by using azo dye **1a** and amine (2-aminobenzimidazole). Dark brown powder; 78%; dp 261 ºC. IR *ν* (cm^{-1}): 3442 (O–H), 3353 (N–H), 3076 (Ar–H), 2881 (C–H), 1681 (CH=N), 1622 (C=C), 1557 (C=N, ring), 1514 (N=N), 1475 (NO_2 asym), 1339 (NO_2 sym), 1244 (C–O). ^{1}H NMR *δ* (ppm): 6.50 (s, 2H, NH, benzimidazole), 6.84–6.87 (m, 4H, benzimidazole), 7.09–7.12 (m, 4H, benzimidazole), 7.41–7.45 (d, 1H, Ar-H), 7.51 (s, 1H, Ar–H), 7.61 (s, 2H, Ar–H), 7.71 (s, 1H, Ar–H), 7.93 (s, 1H, Ar–H), 8.03 (s, 1H, Ar–H), 8.30 (s, 2H, CH=N), 9.63 (s, 2H, OH). ^{13}C NMR *δ* (ppm): 111.82, 115.72, 119.28, 119.54, 119.81, 120.07, 121.72, 122.58, 123.36, 125.61, 130.29, 134.37, 136.29, 137.69, 146.45, 154.42 (Ar–C), 155.28 (C–OH), 159.64 (C=N, benzimidazole), 163.80 (CH=N). UV–Vis (DMSO, 30 µM): λ_{max} (nm): 288, 398 (logε = 4.63, 4.39). Anal. calcd. for ($C_{34}H_{21}Cl_2N_{11}O_4$) (718.51 g/mol): C, 56.83%; H, 2.95%; N, 21.44%. Found: C, 56.55%; H, 2.89%; N, 20.93%. MS (ESI+): *m/z* = 716.8432 $[(M - H)]^+$, calcd. 716.1077 $[(M - H)]^+$.

6,6'-((2-nitro-1,4-phenylene)bis(diazene-2,1-diyl))bis(2-(((1H-imidazol-4-yl)methylene)amino)-4-chlorophenol (2b). The product was obtained by using azo dye **1b** and aldehyde (4-imidazolecarboxaldehyde). Dark brown powder; 89%. dp 243 ºC. IR *ν* (cm^{-1}): 3462 (O–H), 3344 (N–H), 3120 (Ar-H), 2837 (C–H), 1666 (C=N), 1625 (C=C), 1587 (C=N, ring), 1564 (N=N), 1510 (NO_2 asym), 1337 (NO_2 sym), 1247 (C–O). ^{1}H NMR *δ* (ppm): ^{1}H NMR *δ* (ppm): 6.34 (s, 2H, NH, imidazole), 7.02 (s, 2H, Ar-H), 7.17 (s, 2H, imidazole), 7.38 (s, 1H, Ar–H), 7.50 (s, 1H, Ar–H), 7.66 (s, 2H, imidazole), 7.71 (s, 1H, Ar–H), 7.92–7.99 (d, *J* = 27.33, 1H, Ar–H), 8.44 (s, 1H, Ar–H), 8.66 (s, 2H, CH=N), 9.74 (s, 1H, OH, azo-imine tautomer), 12.81 (s, 1H, NH, hydrazone-imine tautomer). ^{13}C NMR *δ* (ppm): 115.57, 116.83, 117.15, 117.54, 119.16, 125.35, 126.65, 128.69, 129.09, 134.44, 135.67, 140.98, 147.83, 149.08 (Ar–C), 154.31 (C=N, imidazole), 156.45 (CH=N), 172.02 (C–OH). UV–Vis (DMSO, 30 µM): λ_{max} (nm): 396 (logε = 4.63). Anal. calcd. for ($C_{26}H_{17}Cl_2N_{11}O_4$) (618.39 g/mol): C, 50.50%; H, 2.77%; N, 24.92%. Found: C, 50.42%; H, 2.68%; N, 25.03%. MS (ESI+): *m/z* = 619.5233 $[(M + H)]^+$, calcd. 620.0886 $[(M + H)]^+$.

3. THE RESEARCH FINDINGS AND DISCUSSION

3.1. Synthesis and Characterization

The azo coupling reaction of 2-nitro-1,4-phenylenediamine with 5-chlorosalicylaldehyde and 5-chloro-2-hydroxyaniline produced azo-aldehyde (**1a**) and azo-amine (**1b**) dyes, respectively. Corresponding Schiff base derivatives (**2a-b**) were newly obtained through the reaction of 1 equiv of azo dyes with 2 equiv of 2-aminobenzimidazole and 4-imidazolecarboxaldehyde (Figures 1-2). In this work, these substances were

reported for the first time. They were explicitly identified by infrared, nuclear magnetic resonance, mass and absorption spectroscopies (Supplemental Figures S1-S16). The obtained microanalysis results are in agreement with the calculated elemental values. New substances are dark brown colored, soluble in organic solvents and stable in air.

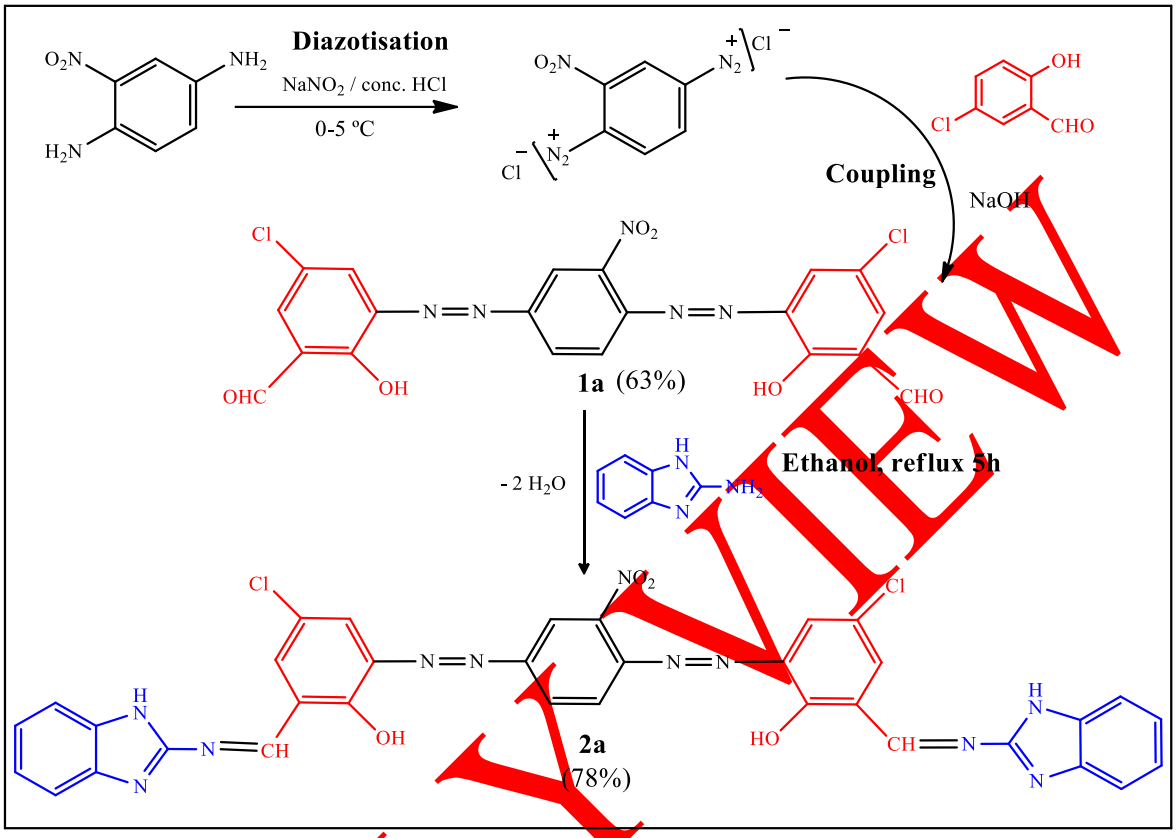

Figure 1. *Synthesis diagram of azo-aldehyde dye (**1a**) and Schiff base derivative (**2a**)*

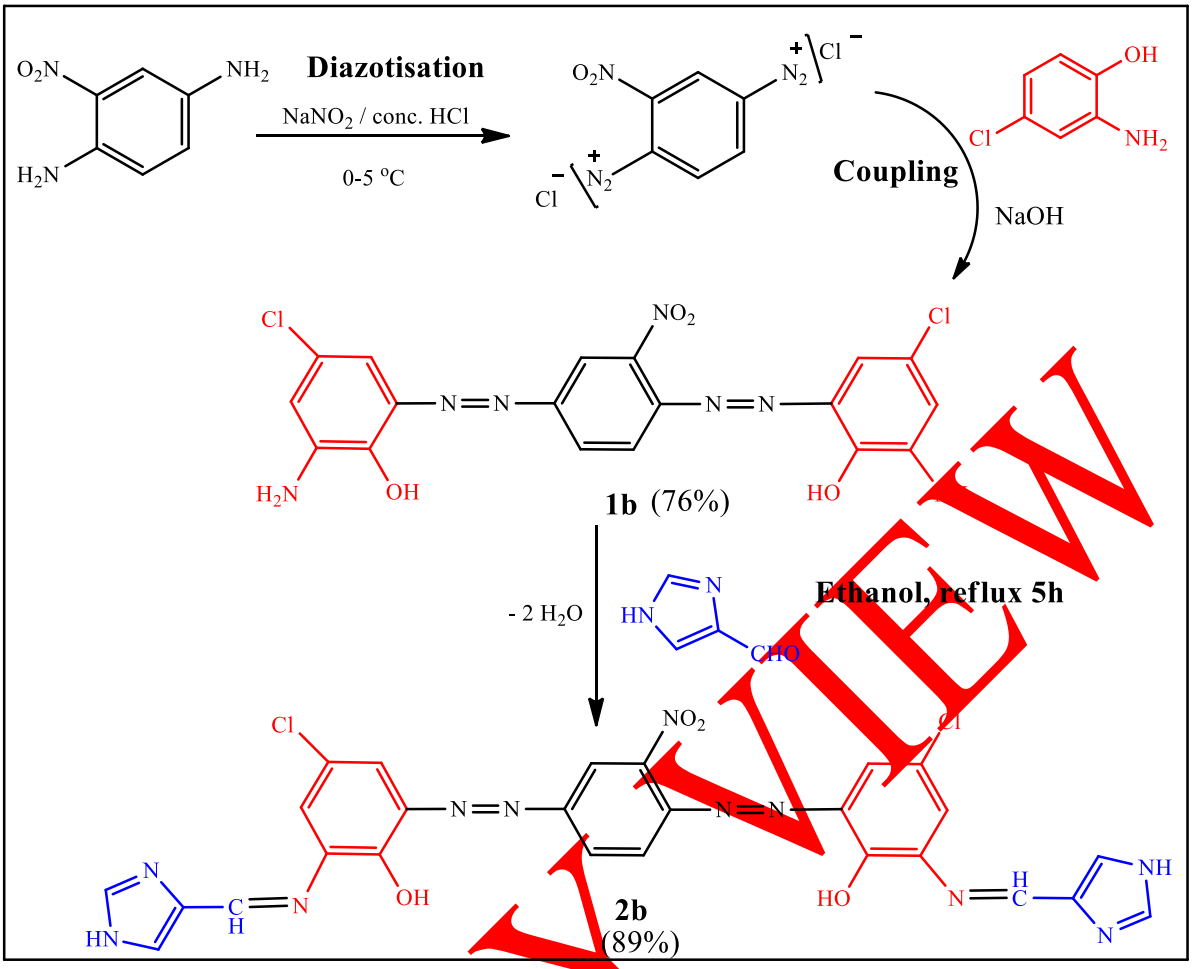

Figure 2. *Synthesis diagram of azo-amine dye (**1b**) and Schiff base derivative (**2b**)*

It is well known that in Schiff bases and azo dyes containing OH group at ortho-position of phenyl rings, the polar electron–donating OH groups lead to form an intramolecular H-bond between enol-imine ↔ keto-amine and azo ↔ hydrazone tautomeric forms, respectively. Tautomeric equilibrium of azo-Schiff bases **2a-b** is given in Figure 3 and Supplemental Figure S17.

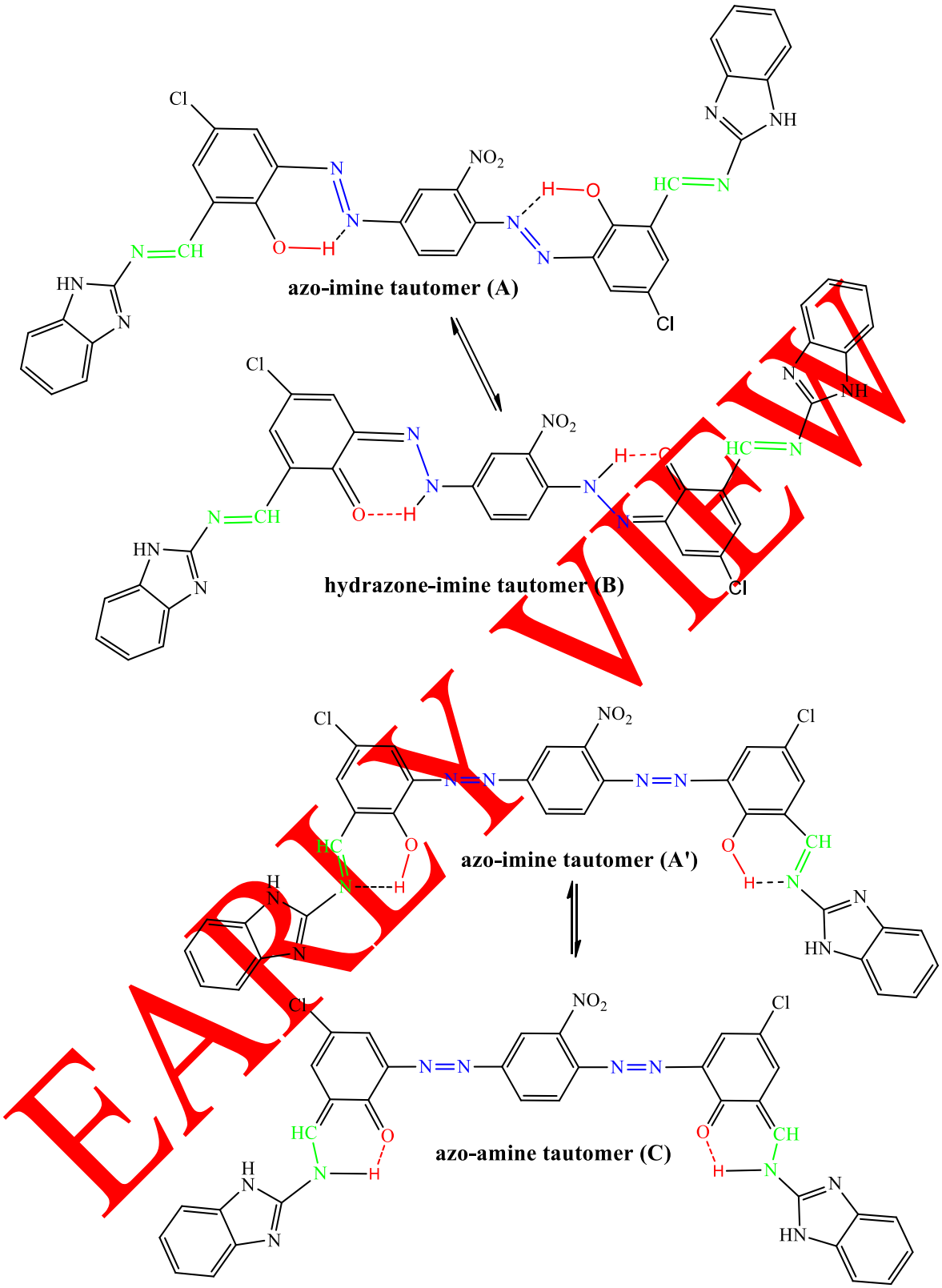

Figure 3. *The proposed tautomeric equilibria in* ***2a***

In FT–IR spectrum of azo dyes, the *v*OH peaked at 3217 cm^{-1} for **1a**, and 3452 cm^{-1} for **1b**. The aldehyde *v*(C–H) and *v*(C=O) frequencies appeared at 2876 and 1679/1656 cm^{-1} for **1a**. The dual band at 3346/3184 cm^{-1} was due to the *v*NH frequency of **1b**. The azo *v*(N=N) frequency appeared at 1529 cm^{-1} for **1a** and 1563 cm^{-1} for **1b**. The symmetric and asymmetric *v*(NO_2) frequencies were observed at 1469/1345 cm^{-1} for **1a** and 1509/1339 cm^{-1} for **1b**. Benzene *v*(C–H) and *v*(C=C) frequencies were at 3076 cm^{-1} and 1613

cm^{-1} for **1a**, and 3087 cm^{-1} and 1624 cm^{-1} for **1b**. The frequency at 1262 and 1246 cm^{-1} was belonged to ν(C–O) of phenol ring for **1a** and **1b**. The νOH frequency centered at 3442 and 3462 cm^{-1} for **2a** and **2b**, respectively. The νNH vibration frequency of imidazole ring peaked a 3353 and 3344 cm^{-1} as a broad band for **2a** and **2b**. The stretching vibration bands due to the aldehyde group disappeared for **2a**. The band at 1681 and 1666 cm^{-1} was corresponded to the ν(C=N) frequency of the imine group for **2a** and **2b**, respectively [39], showing Schiff base formation through a condensation reaction. The frequency at 1557 and 1587 cm^{-1} was attributed to C=N group of imidazole for **2a** and **2b**, respectively [40]. The vibration band at 1514 and 1564 cm^{-1} was due to ν(N=N) frequency of azo group for **2a** and **2b**. The nitro frequencies were at 1475 and 1339 cm^{-1} for **2a**, and 1510 and 1337 cm^{-1} for **2b**. The (C–O) band was at 1244 and 1247 cm^{-1}. These results indicated that **2a** and **2b** most likely exist as a mixture of azo and imine tautomer in the solid state.

In ^{1}H NMR spectrum of **1a**, the aldehyde (CHO) proton was observed at δ_H 10.21 ppm as a singlet signal. The phenolic OH proton was seen at δ_H 10.06 and δ_H 10.09 ppm for **1a** and **1b**, respectively. Free amino protons of **1b** appeared at δ_H 6.34 ppm. Benzene protons resonated in the range of δ_H 7.53–8.25 ppm and δ_H 7.24–8.38 ppm for **1a** and **1b**, respectively. For **2a**, the aldehyde proton signal was absent. The singlet peak at δ_H 8.30 ppm for **2a** and δ_H 8.66 ppm for **2b** was attributed to (CH=N) proton [41]. The OH proton signal shifted to upfield compared to that of corresponding azo compounds. It was observed at δ_H 9.63 and δ_H 9.74 ppm for **2a** and **2b**, respectively. These results confirmed that **2a** and **2b** exhibit as azo-imine tautomer in DMSO solution. On the other hand, the singlet at δ_H 12.81 ppm may be corresponded to the NH proton of hydrazone-imine tautomeric form of **2b** (Supplemental Figure S17). The proportion of azo-imine tautomer in this compound can be calculated by the intensities of δ_{OH} *and* δ_{NH} shifts values of the corresponding tautomeric forms. The intensity of the OH proton signal is 1.84, and the intensity of the NH proton signal is 0.30, then the percentage of azo form is close to ~86%. One-proton singlets at δ_H 6.50 ppm and δ_H 6.34 ppm may be attributed to the NH proton of imidazole ring for **2a** and **2b**, respectively [42,43]. Benzene signals were recorded within the range of δ_H 7.41–8.03 ppm and δ_H 7.02–8.44 ppm for **2a** and **2b**. Benzimidazole signals were seen at δ_H 6.84–6.87 and δ_H 7.09–7.12 ppm as multiplet and doublet peaks for **2a**. Imidazole protons appeared at δ_H 7.17 and δ_H 7.66 ppm as a singlet signal for **2b**.

^{13}C NMR spectrum of **1a** exhibited the aldehyde (CH=O) and the (C-OH) carbons at δ_C 189.83 and δ_C 159.39 ppm. The azo-linkaged (C–N=N) aromatic carbons displayed two different signal at δ_C 157.82 and δ_C 149.96 ppm. The nitro-substituted (C–NO_2) aromatic carbon resonated at δ_C 144.17 ppm. For **1b**, the phenolic (C–OH) carbon signalized at δ_C 153.00 ppm. The azo-linkaged carbons appeared at δ_C 149.25 and δ_C 148.07 ppm. The nitro-substituted carbon was seen at δ_C 140.89 ppm, respectively. Other benzene carbons were seen between δ_C 119.60 and 137.64 ppm for **1a**; δ_C 117.80 and 135.88 ppm for **1b**. In ^{13}C NMR spectrum of **2a**, the aldehyde carbon signal disappeared. The new peak at δ_C 163.80 was assigned to the imine (CH=N) carbon atom [44]. Benzimidazole (C=N) carbon resonated at δ_C 159.64 ppm. The phenolic (C–OH) carbon signal gave upfield shifting to 155.28 ppm. The azo-linkaged carbons signalized at δ_C 154.42 and δ_C 146.45 ppm. The nitro-substituted carbon was observed at δ_C 137.69 ppm. For **2b**, the imine and imidazole (C=N) carbons were seen at δ_C 156.45 and δ_C 154.31 ppm. The phenolic (C–OH) carbon signal shifted downfield to 172.02 ppm. The (C–N=N) and (C–NO_2) carbons were at δ_C 149.08/147.83 and δ_C 140.98 ppm.

In mass spectrum of **1a**, high relative intensity peak was seen by the reduction of chlorine atom of molecule at *m/z* 452.5663. This fragment was followed by loss of ($C_7H_4NO_2$) radical and showing the strong peak at *m/z* 321.3554. The mass spectral pattern of **1b** exhibited the peaks at *m/z* 425.3163 and 319.2327, which are corresponded to loss of chlorine atom and (C_6H_5NO) radical, respectively. Compound **2a** displayed $[M-H]^+$ ion peak at *m/z* 716.8432. The following fragment appeared at *m/z* 507.3954 by loss of two chlorine atoms and ($C_8H_6N_3$) radical. In the presence of **2b**, $[M+H]^+$ ion peak was recorded at *m/z* 619.5233. This fragment was followed by loss of chlorine atom and ($C_4H_4N_3$) radical giving the peak at *m/z* 483.4228. High relative intensity peak at *m/z* 275.1811 may be corresponded to ($C_{16}H_{11}N_5$) radical.

3.2. Donor–(π–Electron Bridge)–Acceptor Structure of Azo-Schiff Bases (2a-b)

Polyaromatic planar heterocyclic D–π–A molecules have extensive π-electronic delocalization system between donor and acceptor units. These chromophores present variety of photophysical transfer mechanisms like as intra/intermolecular charge (ICT), intramolecular proton in excited state (ESIPT) and photoinduced electron (PET) [45]. ICT mechanism is related to HOMO of donor and LUMO of acceptor, and the linker that connect both. Charge transfer directly associates with the ionization energy of donor unit. An ESIPT active molecule must iclude both an acidic (H–donor) and basic (H–acceptor) sites or in close proximity. For PET mechanism, electron transfer occurs between donor and acceptor units of the molecule in excited state via non-radiative pathway [46].

Azo-Schiff bases (**2a-b**) developed as D–π–A molecular systems have similar pheny/phenyl/heteroaromatic ring skeletal structure linked by azo and imine double bonds (Figure 4). The presence of electron–withdrawing nitro group and chlorine atoms at meta-position of phenyl rings provides the push-pull tuning (unsymmetrical electron distributions) property of the molecules. Tertiary imidazole (C=N) nitrogen atom of benzimidazole and imidazole rings acts as an electron-donating cores. The lone pair electrons of pyrrole (NH) nitrogen atom in benzimidazole ring are delocalized with the π system of aromatic ring. Stabilization of the whole molecule is due to interaction between electron-acceptors and electron-donors. Effective and intensive π-π conjugation of azo and imine bonds is achieved by intramolecular charge transfer from π-donor to π*-acceptor. The molecular conjugation is also achieved by the introduction of salicylidene moieties.

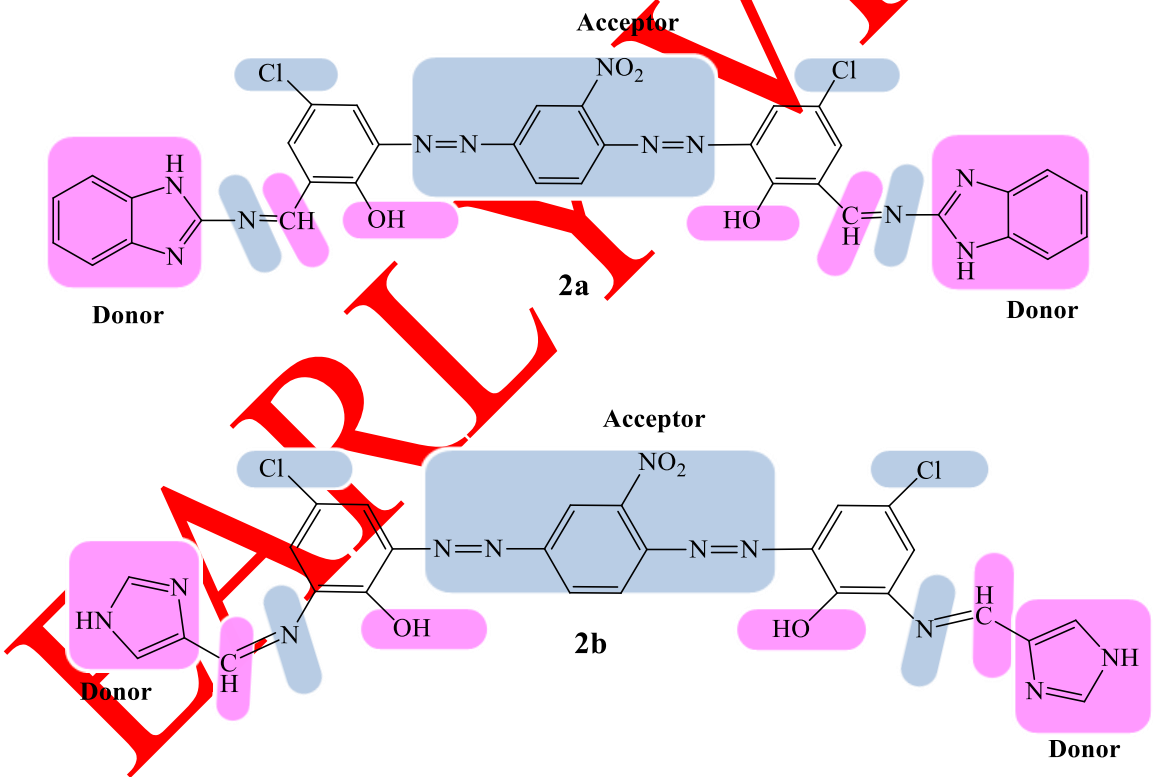

Figure 4. *Donor–π–acceptor molecular structure of azo-Schiff bases (**2a-b**)*

3.3. Structure Effect on Electronic Absorption Spectra

2a and **2b** are expected to display two main transitions: π→π* and n→π*. The main absorption bands originate from π–conjugation system transitions of azo and imine bonds. HOMO→LUMO (π→π*) transitions can also represent intraligand charge transfer bands from phenyl to phenyl ring, benzimidazole/imidazole to phenyl ring or electron-withdrawing groups at the phenyl towards benzimidazole/imidazole ring of the molecule.

In DMSO, **2a** bearing benzimidazole ring exhibited two absorption maximum at 282 and 401 nm, while **2b** including imidazole ring had only one maximum at 396 nm (Figure 5). In DMF, **2a** showed the bands at 287 and 394 nm, **2b** had a main band at 393 nm. In $CHCl_3$, the bands were recorded at 257, 278 and 383 nm for **2a**; 262 and 387 nm for **2b**. The wavelength of higher energy bands was belonged to phenyl ring π→π* transition [47]. The broad overlapping band above 380 nm may belong to to a combination of imine n→π* and azo π→π* transitions. The shoulder at 325 nm for **2a** was corresponded to (C=N) bond π→π* transition of benzimidazole ring. This transition may become more strongly with respect to the resonance effect of extra phenyl ring, which is not present in **2b**.

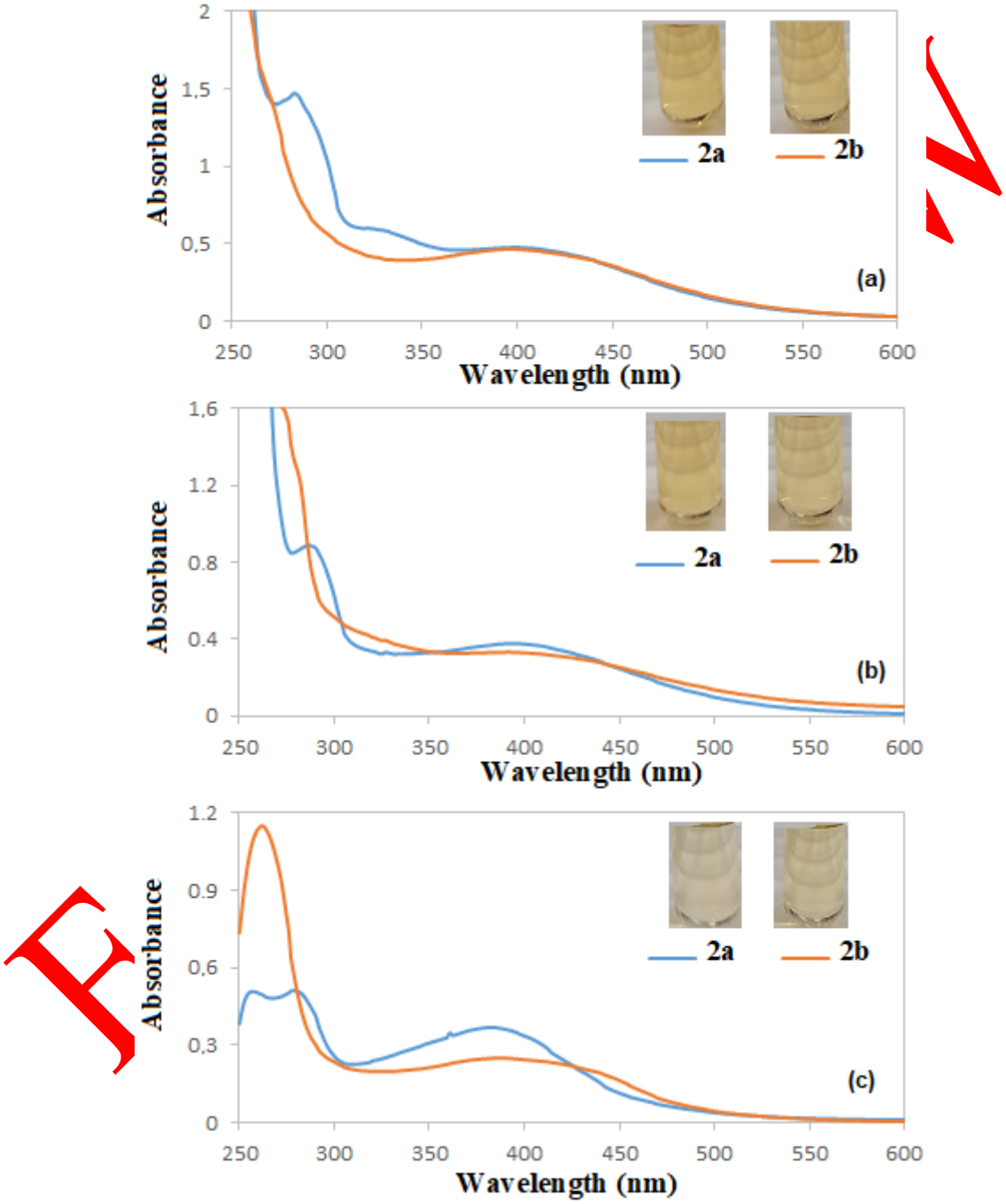

Figure 5. *Electronic absorption spectra of* ***2a*** *and* ***2b*** *in DMSO* ***(a)****, DMF* ***(b)*** *and* $CHCl_3$ ***(c)***

For Schiff bases derived from salicylaldehyde, the relative stability of keto-amine tautomer decreases because of lossing of aromaticity [1]. Hydrazone tautomer generally absorbs at longer wavelengths than azo tautomer, and it has better dyeing power. UV–Vis data of **2a** and **2b** showed that all the bands are seen

at lower wavelength. This finding confirmed that these compounds mainly exist as azo-imine tautomer in solution. The existence of lowest energy transition bands below 400 nm may be explained by the induction effect of *O* and *N* atoms in structure. Presence of intramolecular hydrogen bonding between imine and (OH) group causes a blue-shift in this absorption band. Bathochromic and hypsochromic shifts in absorption bands can also be dependent on a weak mesomeric electron-repulsive and a strong inductive electron-withdrawing characters of chlorine atoms and electron-attracting effect of nitro group at meta-position of phenyl rings [48,49]. Delocalization of the lone pair electrons of *N* atom of azo chromophore is hinder by electron-withdrawing character of Cl substituent. Moreover, the formation of a strong π charge delocalization between azo/imine chromophores and aromatic/heteroaromatic rings leads to decrease in the absorption wavelength. Substitution of imidazole of **2b** with benzimidazole (**2a**) affects a larger delocalized π-electron system over phenyl and salicylidene rings.

3.4. Solvent Effect on Electronic Absorption Spectra

The solvent polarity strongly effects the excited state of D–π–A molecule by stabilizing it via solvation, dipole-dipole interactions and formation of stronger intermolecular H-bonding. As seen in Figure 5, the solution colors turned from orange to colorless with changing of polarity. The absorption spectrum of **2a** displayed the bands at 282, 325(sh) and 401 nm in DMSO (ε = 46); 287 and 394 nm in DMF (ε = 37); 257, 278 and 383 nm in $CHCl_3$ (ε = 4.8). When the dielectric constant (ε) of solvents increased, the third band shifted bathochromically ($\Delta\lambda_{max}$ = 7–18 nm) (positive solvatochromism). Aswell, hyperchromic effect was noted for the absorbance of the first transition, which decreases in the order of DMSO > DMF > $CHCl_3$. The shoulder related to π→π* transition of $(C{=}N)_{benzimidazole}$ appeared in only protophilic DMSO solution. This transition may be stabilized via H-bonding between double bonded *O* atom of dipolar aprotic protophilic DMSO molecule and (NH) proton of benzimidazole rings. In the presence of **2b**, decreasing of solvent polarity caused that the color of solutions turns to light yellow. **2b** had the band at 396, 393, and 262 and 387 nm in these solutions, respectively. This broad band red-shifted to longer wavelength (bathochromic shift) ($\Delta\lambda_{max}$ = 3–9 nm), and the absorbance increased with increasing of dielectric constant of solvents (positive solvatochromism).

It has been determined that the stability of tautomers depends on temperature and solvent [50,51]. Enol-imine form becomes more stable in polar solvents [52,53]. The obtained results indicated that the absorption band positions of **2a** and **2b** show a major dependence on solvent polarity. In polar solvents, intramolecular hydrogen bonding interaction between imine and the hydroxyl groups completely disappear or weakened, so the absorption band corresponded to n→π* transition of imine shows a red-shift [44]. Positive solvatochromism suggests that polar solvents stabilize excited state more than the ground state [54]. This may be due to the effect of changes of dipole moment, protonation and H–bonding strength upon electronic excitation [55]. In inert $CHCl_3$, π→π* transition of phenyl ring became more stable, which is resulted that higher energy band is observed at 257 and 262 nm for **2a** and **2b**.

3.5. Acid–Base Effect on Electronic Absorption Spectra

Azo-Schiff bases (**2a**-**b**) have both deprotonable acidic (OH and $NH_{imidazole}$) and protonable basic (azo, imine and $imino_{ring}$) active cores. Benzimidazole and imidazole ring system is amphoteric, they act as both acid and base due to proton releasing and binding property of pyrrole and tertiary imidazole nitrogen atoms in their molecular structure. Since their basic character is slightly higher than acidic property, they can form salts with acids. Benzimidazole acts as weaker base than imidazole, related to the conjugation between imidazole and benzene rings in its structure. On the other hand, substituents in salicylidene and phenyl rings influence protonation equilibrium by increasing basicity of azo and imine chromophores or increasing acidity of the phenolic group, depending on their steric and electronic effects.

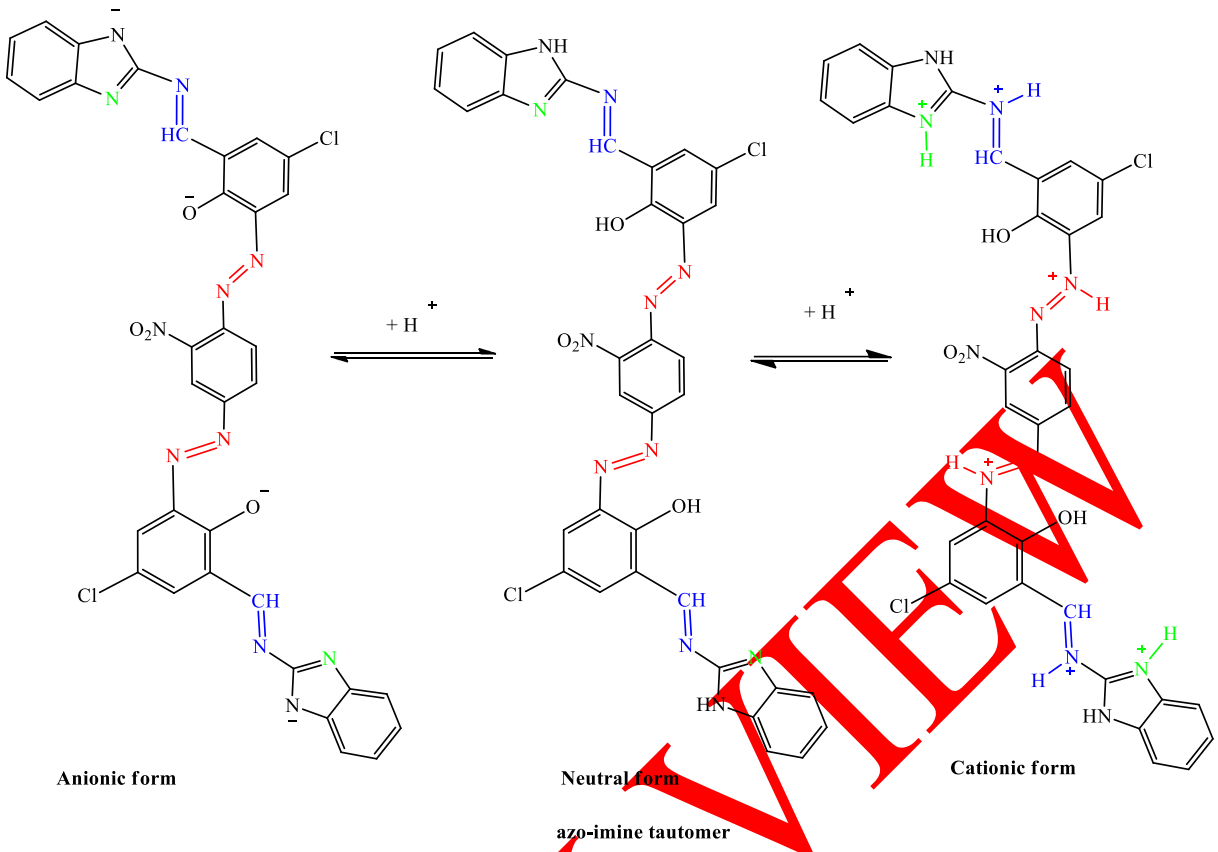

Figure 6. *Acid and base equilibrium in* ***2a***

In the synthesized azo-Schiff bases, protonation can occur on azo, imine and imidazole nitrogen atom of imidazole moiety, that leads to formation of dicationic, tetracationic and hexacationic forms in solution. This protonation equilibrium is depicted in Figure 6 and Supplemental Figure S18. When DMSO and DMF solution of **2a** was strongly acidified with aqueous HCl solution, orange color changed to light yellow (positive acidochromism). In acidic DMSO, the first λ_{max} value shifted hypsochromically to 277 nm. The hump band (due to $(C=N)_{benzimidazole}$) displayed small bathochromic shift ($\Delta\lambda_{max} \sim 6$ nm). The λ_{max} value of the third band (due to azo/imine chromophores) showed small hypsochromic shift ($\Delta\lambda_{max} \sim 19$ nm) (Figure 7). Protonation of **2a** caused a decrease in molar extinction coefficient of the bands. In acidic DMF, the bands hypsochromically shifted to 280 and 389 nm. For **2b**, orange color solution turned to light yellow–colorless in acidic DMSO and DMF media. Protonation of **2b** caused a blue-shift absorption wavelength (λ_{max} = 396 to 385 nm in DMSO, 393 to 386 nm in DMF). Absorption maxima was newly observed between 274 and 279 nm (Figure 8).

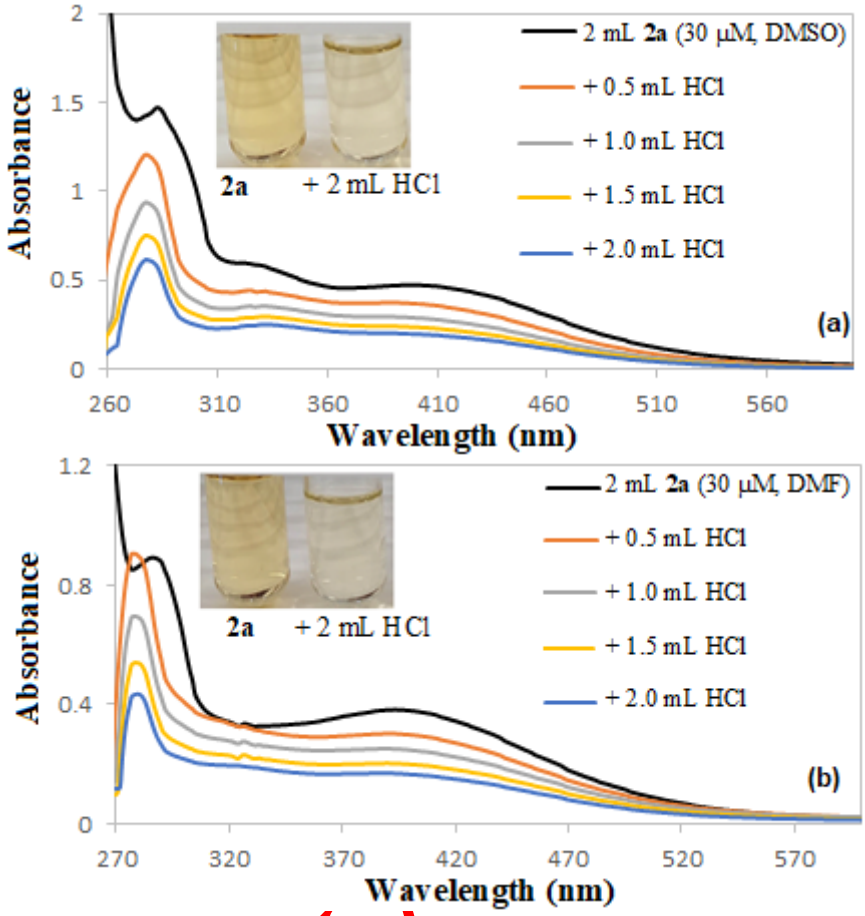

Figure 7. *Electronic absorption spectra of* ***2a*** *upon addition of aqueous HCl solution*

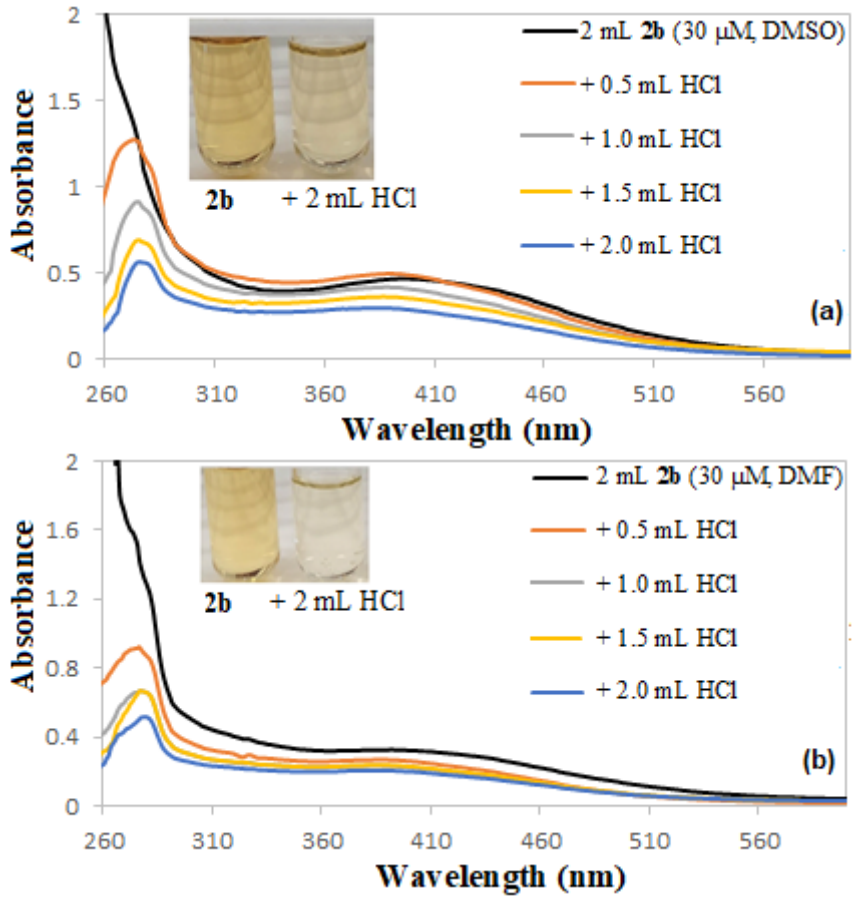

Figure 8. *Electronic absorption spectra of* ***2b*** *upon addition of aqueous HCl solution*

Adding of aqueous NaOH solution to DMSO solution of **2a** caused the significant photophysical changes in the spectrum (Figure 9). Upon the addition of ~0.25 equiv of base, a new dual band was seen at 269 and 297 nm, which is due to the presence of negatively-charged anionic species in solution (Supplemental Figure S18). This dual band converted to a maximum at 281 nm, and the shoulder disappeared with increasing volume of base. In basic DMF, the first λ_{max} value bathochromically shifted to 287 nm, showing the deprotonation of OH groups. After the progressive addition of base, a new maxima was seen at 282 nm in DMSO; a new dual band was observed at 282–294 nm in DMF for **2b** (Figure 10). The absorption band (due to azo/imine chromophores) exhibited no shifts for **2a** and **2b** in basic DMSO and DMF.

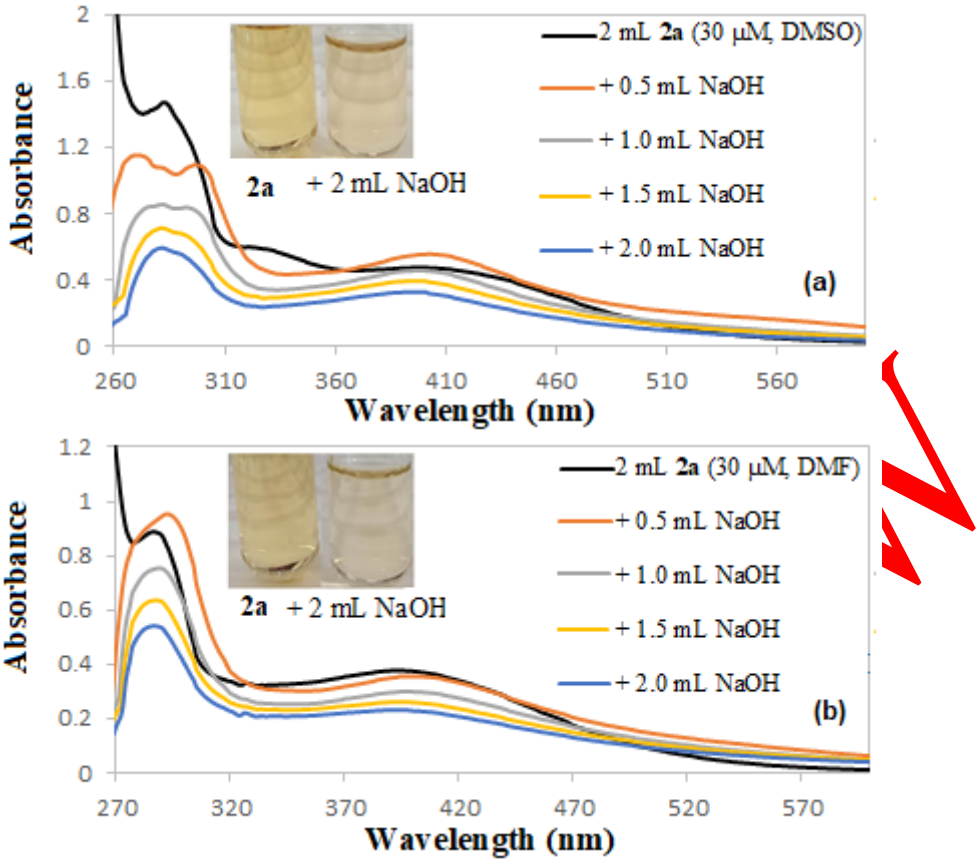

Figure 9. *UV–Vis spectra of **2a** after addition of aqueous NaOH solution*

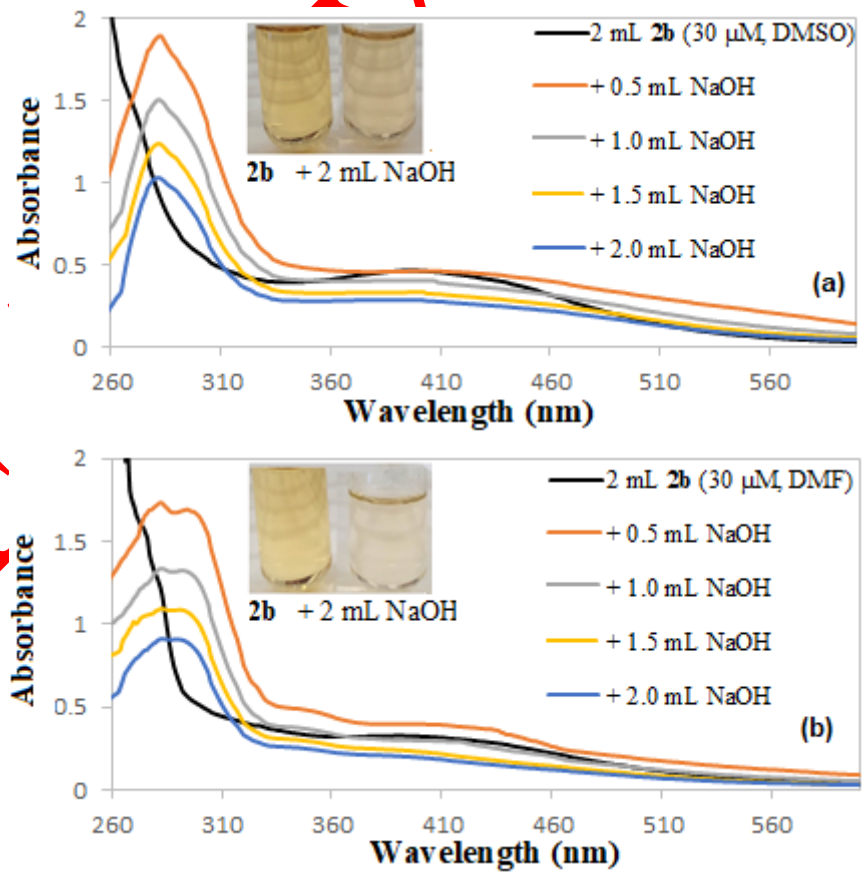

Figure 10. *Electronic absorption spectra of **2b** upon addition of aqueous NaOH solution*

3.6. Temperature Effect on Electronic Absorption Spectra

The electronic absorption spectrum of **2a** and **2b** were also recorded at various temperatures (C = 30 μM). The original spectrum of **2a** exhibited the absorption maxima at 282, 325(sh) and 401 nm; 287 and 394 nm; 257, 278 and 383 nm at room temperature. **2b** had the band at 396 nm in DMSO; 393 nm in DMF; 262 and 387 nm in $CHCl_3$. When these solutions were heated up from 25 ºC to 55 ºC, it was noted that the molar extinction coefficient values of original bands slowly increased (Figures 11-12). Despite of this, there was no change in color of solution and significant shift in spectra, except DMSO. The shoulder was absent in DMSO for **2a**. These results indicated that increasing of temperature only stabilized azo-imine tautomer in the ground state. Tautomeric equilibrium of **2a** and **2b** were not influenced by the change of temperature.

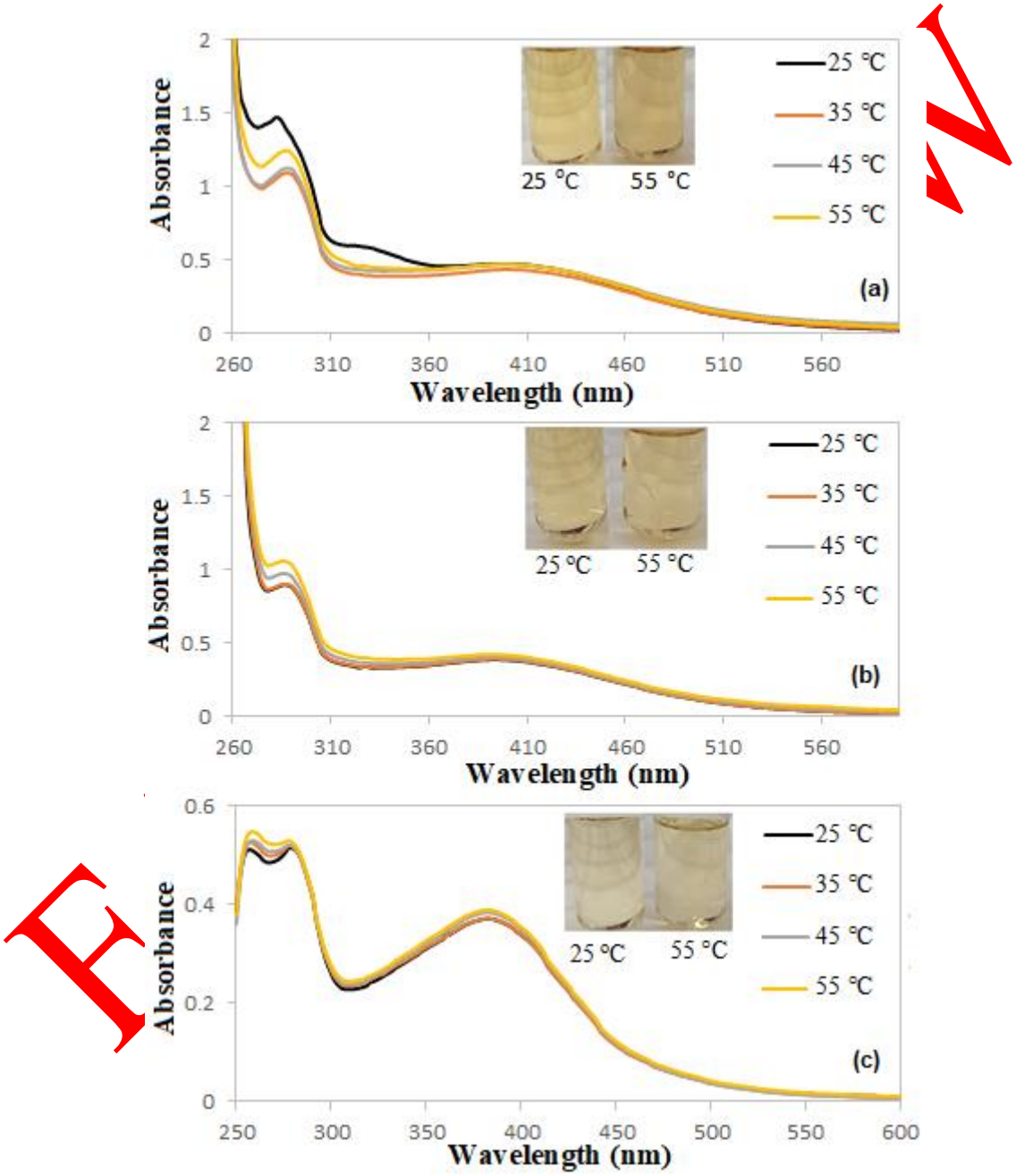

Figure 11. *Electronic absorption spectra of **2a** in DMSO **(a)**, DMF **(b)** and $CHCl_3$ **(c)** at different temperature values*

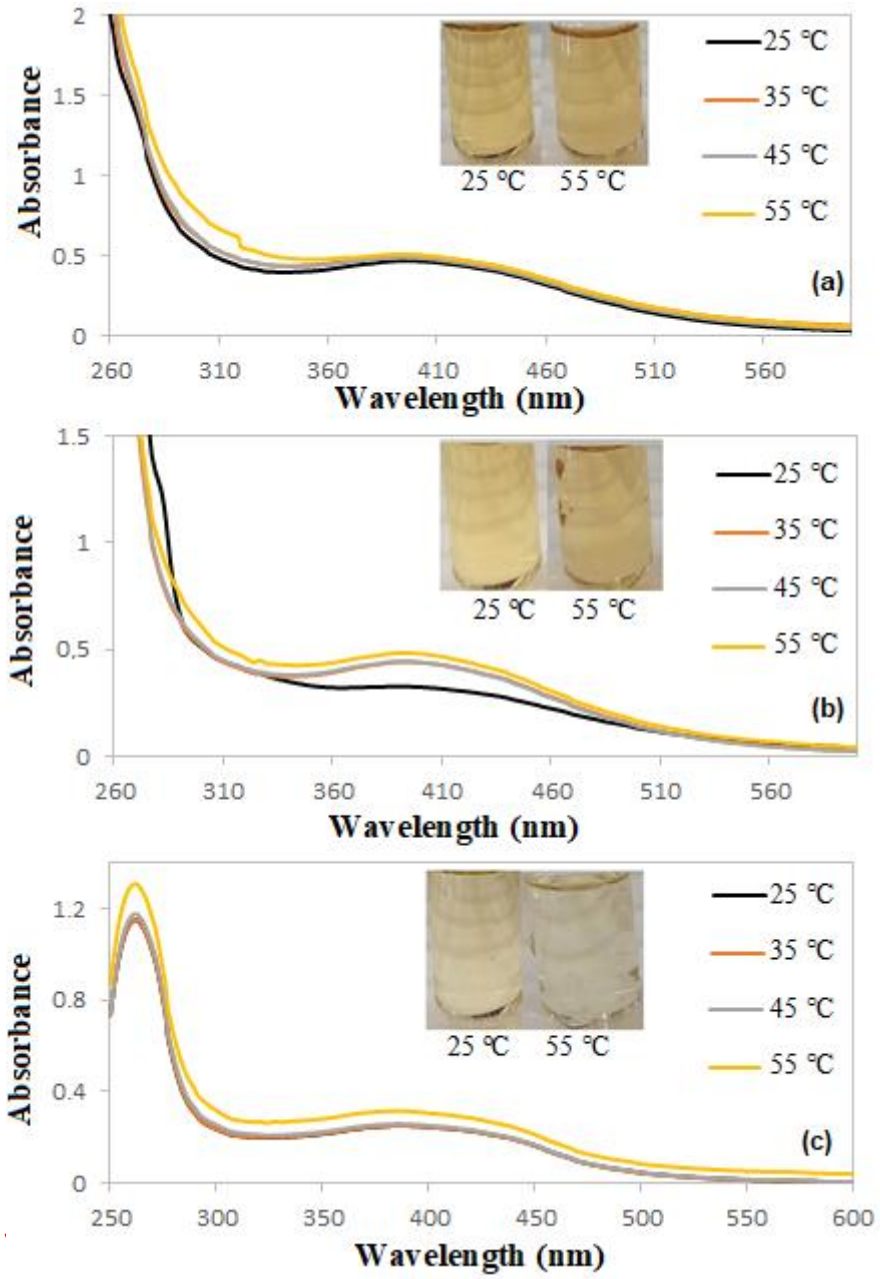

Figure 12. *Electronic absorption spectra of* ***2b*** *in DMSO* ***(a)****, DMF* ***(b)*** *and* $CHCl_3$ ***(c)*** *at different temperature values*

3.7. Structure Effect on Emission Spectra

It is reported that salicylideneaniline Schiff bases and azobenzenes undergo intramolecular proton transfer reaction in excited state upon treating with photon, which results phototautomerization process and is characterized by a large Stokes shift. The types of emission bands for azo dyes and Schiff bases are depicted in Supplemental Figure S19. Higher energy first band is assigned to normal-form (N*). This is generally seen in polar or protic solvents. The lower energy extra band is belonged to tautomeric-form (T*) in excited state. This can be observed in apolar or hydrocarbon solvents [56]. Luminescence emission originates from keto-amine and hydrazone tautomers at low temperatures [57].

Photoluminescence spectra of 2a and 2b were recorded in DMSO, DMF and $CHCl_3$ (C = 30 μM) after excitation at λ_{exc} = 325 nm. In these solutions, the excitation band appeared at λ_{exc} = 413–417 nm for **2a** and λ_{exc} = 405–421 nm for **2b**. In DMSO, turquoise luminescence was observed with the emission bands

centered at λ_{em} = 485 nm for **2a** including benzimidazole moiety (Figure 13). This band red-shifted to λ_{em} = 505 nm for **2b** including imidazole moiety. In DMF, the emission bands appeared at λ_{em} = 499 nm for **2a**, and λ_{em} = 501 nm for **2b**. In $CHCl_3$, the emission band was located at λ_{em} = 503 nm for **2a**. This band shifted to λ_{em} = 509 nm for **2b**. The luminescence intensity of **2b** was observed to be 1.22-fold lower than that of DMSO solution of **2a**. But, it was found to be 2.02-fold and 1.21-fold stronger than that of DMF and $CHCl_3$ solution **2a**, respectively. The decreased in intensity may be explained by π–electron delocalization within the system for **2a**.

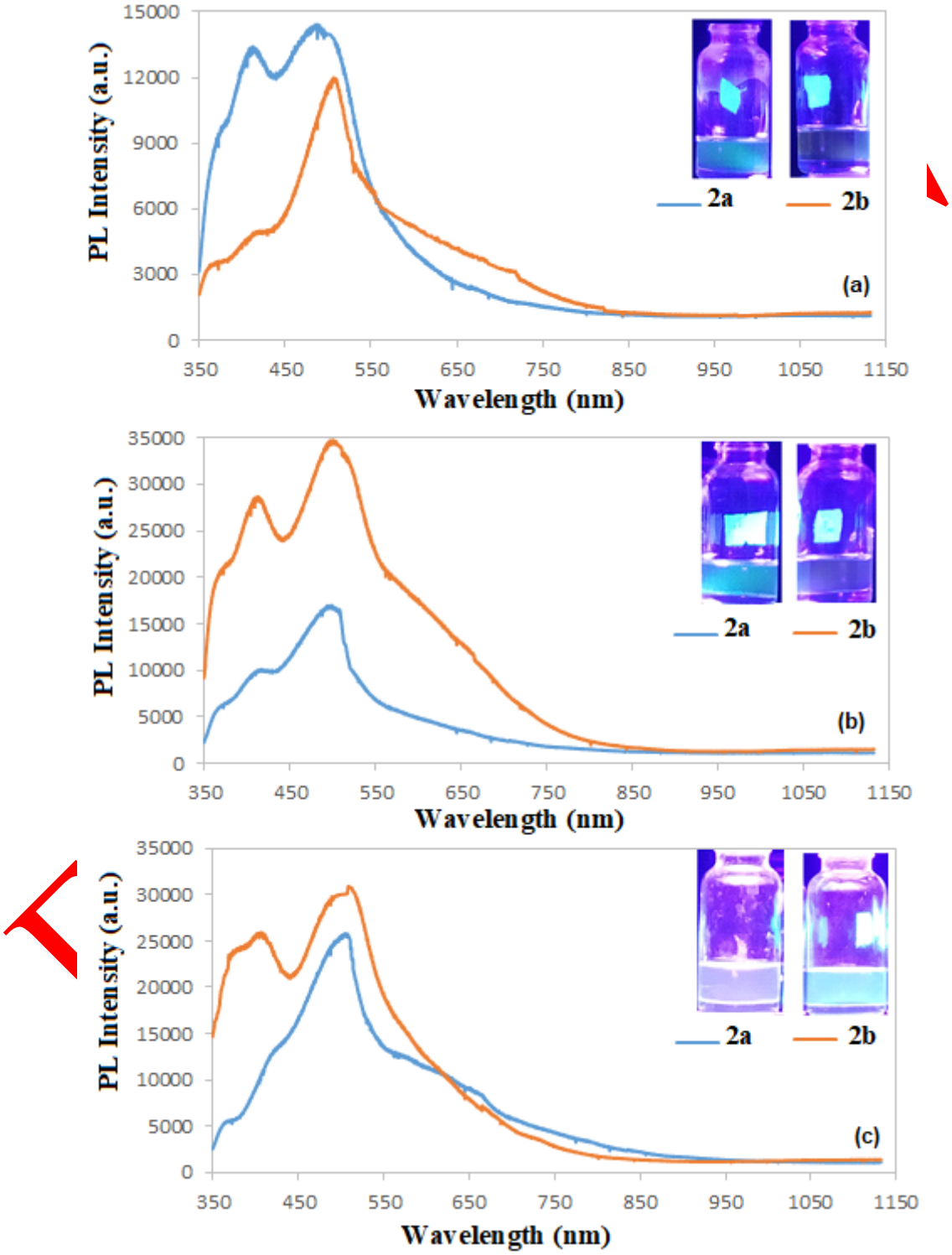

Figure 13. *Photoluminescence spectra of **2a** and **2b** in DMSO **(a)**, DMF **(b)** and $CHCl_3$ **(c)**. Insets: the photograph of the compounds upon excitation ($\lambda_{exc.}$ = 325 nm)*

The obtained spectral results indicated that **2a** and **2b** have azo-imine form in the ground state. They were characterized by the emission bands around 485–503 nm and 501–509 nm. These bands may be belonged to $\pi\rightarrow\pi^*/n\rightarrow\pi^*$ transitions from phenyl to phenyl ring, benzimidazole to phenyl ring (**2a**), imidazole to phenyl ring (**2b**). For these heteroarylazo Schiff bases, it was noted that strong electron-acceptor nitro group and extending conjugation system represent enhancement of intramolecular charge transfer effect in excited state. Electron-withdrawing groups stabilize LUMO level of molecule, that cause a decrease in the electronic transition energy and the luminescence intensity.

3.8. Solvent Effect on Emission Spectra

The experimental results showed that dielectric constant of solvents has effect on the intensity, position and shape of emission spectrum of **2a** and **2b**. As shown in Figure 13, **2a** emitted weak turquoise luminescence in DMSO and DMF with 325 nm excitation wavelength, indicating excited state proton transfer reaction (Figure 14). The luminescence band was seen at λ_{em} = 485 nm in DMSO. This band red-shifted to the longer wavelength, and appeared at λ_{em} = 499 nm in DMF. In $CHCl_3$, **2a** displayed white luminescence with emission band at λ_{em} = 503 nm. Herein, it was noted that polarity of solvents leads to a hypsochromic shift for the emission bands (negative solvatochromism), indicating that a weak interaction of polar solvents in the excited state. On the other hand, the luminescence intensity decreased in the order of DMSO > DMF > $CHCl_3$. Observed luminescence of **2a** may prove that azo↔hydrazone tautomeric equilibrium occurs in the excited state. The band around 485–503 nm was due to normal (N*) emission of azo-imine form.

Compound **2b** is non-emissive in DMSO and DMF at room temperature. The formation intermolecular hydrogen bonding between these dipolar aprotic protophilic solvents and the hydroxyl groups of **2b** may hamper ESIPT reaction in the excited state. This resulted that the amount of tautomer (T*) to normal (N*) form dramatically decreases in these solutions. In DMSO, the emission band was centered at λ_{em} = 505 nm (Figure 13). In DMF, a single emission band was located at λ_{em} = 501 nm, which is associated with normal (N*) emission of azo-imine form. In $CHCl_3$, **2b** emitted strong turquoise luminescence with the emission wavelength at λ_{em} = 509 nm. This confirmed that **2b** acts as an ESIPT active luminescent molecule in inert $CHCl_3$.

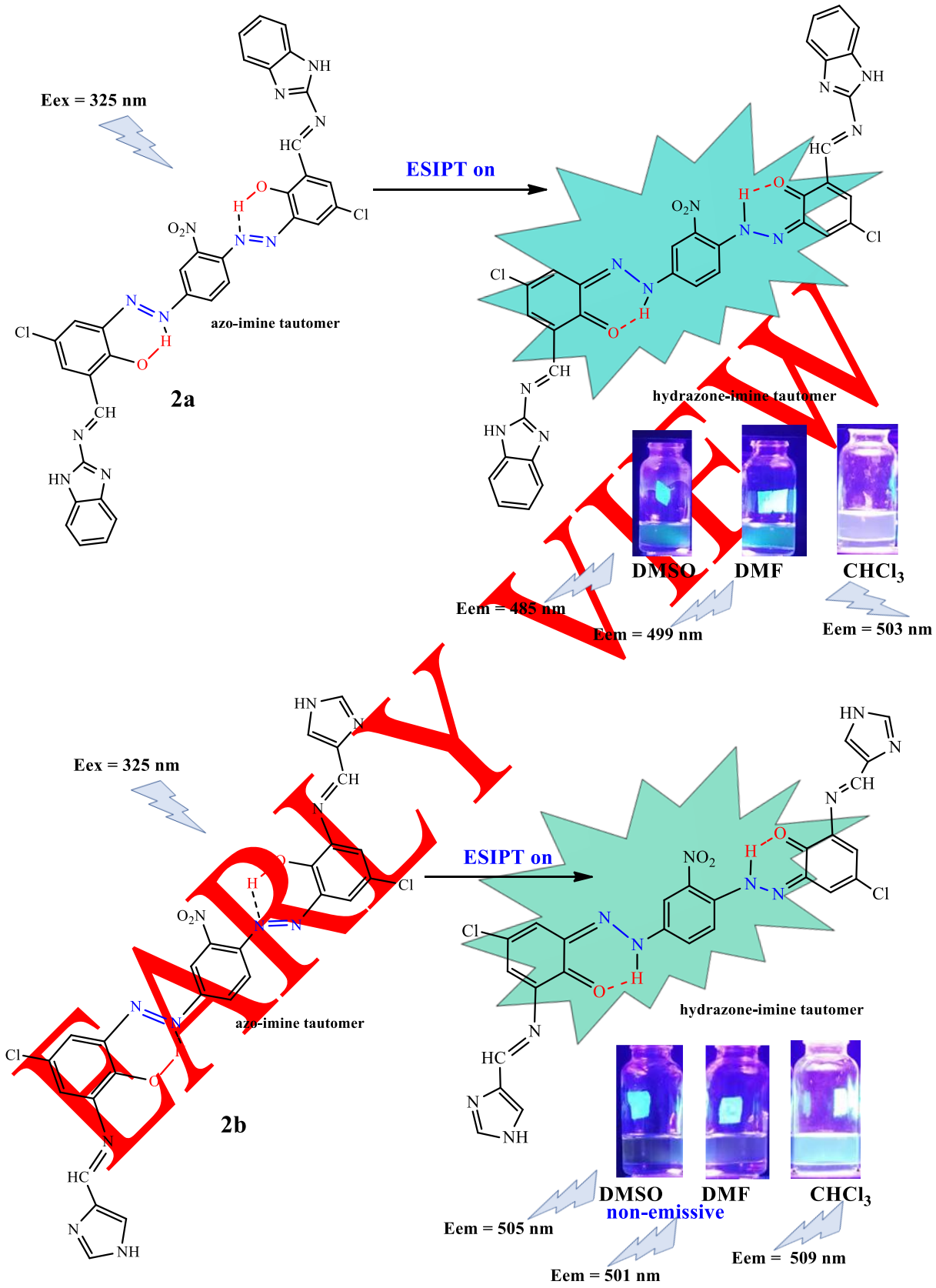

Figure 14. *ESIPT reaction mechanism in azo-Schiff bases (**2a-b**)*

4. RESULTS

Herein, Schiff base derivatives (**2a-b**) having D–π–A system have been produced via the condensation reaction of azo dyes (**1a-b**) with 2-aminobenzimidazole and 4-imidazolecarboxaldehyde. According to FT–IR and NMR spectroscopies, it was noted that a mixture of azo and imine tautomer is mainly presented in solid state and solution in the ground state. In these compounds, prototopic tautomeric equilibria, solvatochromic, acidochromic and thermochromic properties were investigated by UV–Vis spectroscopy. PL spectra were recorded at ambient temperature upon photoexcitation at 325 nm. **2a** showed turquoise luminescence in DMSO and DMF, and white luminescence in $CHCl_3$, but the luminescent efficiency is moderate. **2b** emitted strong turquoise luminescence in $CHCl_3$. This study may offer that luminescent compounds **2a** and **2b** can be utilized as conductive organic material and light emitting diodes for fabricating of new electroluminescent materials. According to the obtained results, this work has significance in molecular design of novel luminescent azo-Schiff bases.

ACKNOWLEDGMENT

I am grateful to Gazi University Research Foundation (Project ID: F.E.F. 05/2019–23). I am also thankful to Gazi University Photonics Application and Research Center for photoluminescence measurements.

CONFLICTS OF INTEREST

No conflict of interest was declared by the author.

REFERENCES

[1] Fita, P., Luzina, E., Dziembowska, T., Kopec, D., Piatkowski, P., Radzewicz, Cz., Grabowska, A., "Keto–enol tautomerism of two structurally related Schiff bases: Direct and indirect way of creation of the excited keto tautomer", Chemical Physics Letters, 416: 305–310, (2005).

[2] Meng, X., Zhu, W., Zhang, Q., Feng, Y., Tan, W., Tian, H., "Novel bisthienylethenes containing naphthalimide as the center ethene bridge: photochromism and solvatochromism for combined nor and inhibit logic gates", The Journal of Physical Chemistry B, 112: 15636–15645, (2008).

[3] Atav, R., Topuz, A., Arıcan, T., "Köpüklü aplikasyon tekniği kullanılarak UV ile renk değiştiren fonksiyonel floklu döşemelik kumaş geliştirilmesi", European Journal of Engineering and Applied Sciences, 1: 15–18, (2018).

[4] Pakolpakçıl, A., Karaca, E., Becerir, B., "Halokromik akıllı tekstil yüzeyleri ve tıbbi amaçlı kullanım olanakları", Journal of Textile Engineering, 25(111): 214–224, (2018).

[5] Açıksarı, C., Karasu, B., "Smart glasses and their technological developments", The El-Cezerî Journal of Science and Engineering, 5(2): 437–457, (2018).

[6] Eren, Z., Acar, F.N., "Uçucu kül adsorpsiyonu ile reaktif boya giderimi", Pamukkale University Journal of Engineering Sciences, 10(2): 253–258, (2004).

[7] Sener, N., Sener, I., Yavuz, S., Karcı, F., "Synthesis, absorption properties and biological evaluation of some novel disazo dyes derived form pyrazole derivatives", Asian Journal of Chemistry, 27: 3003–3012, (2015).

[8] Sheikhshoaie, I., Hossein, M., Mashhadizadeh, Saeid-Nia, S., "Synthesis, characterization and theoretical study of the structure and second-order nonlinear optical properties of two new monoazo Schiff-base compounds", Journal of Coordination Chemistry, 57(5): 417–423, (2004).

[9] Coelho, P.J., Carvalho, L.M., Fonseca, A.M.C., Raposo, M. M. M., "Photochromic properties of thienylpyrrole azo dyes in solution", Tetrahedron Letters, 47: 3711–3714, (2006).

[10] Yılmaz, Z.K., Özdemir, Ö., Aslim, B., Suludere, Z., Şahin, E., "A new bio-active asymmetric-Schiff base: synthesis and evaluation of calf thymus DNA interaction, topoisomerase IIα inhibition, in vitro antiproliferative activity, SEM analysis and molecular docking studies", Journal of Biomolecular Structure and Dynamics, 41: 2804–2822, (2023).

[11] Abdel Aziz, A.A., Badr, I.H.A., El-Sayed, I.S.A., "Synthesis, spectroscopic, photoluminescence properties and biological evaluation of novel Zn(II) and Al(III) complexes of NOON tetradentate Schiff bases", Spectrochimica Acta Part A: Molecular and Biomolecular Spectroscopy, 97: 388–396, (2012).

[12] Raman, N., Selvan, A., Sudharsan, S., "Metallation of ethylenediamine based Schiff base with biologically active Cu(II), Ni(II) and Zn(II) ions: synthesis, spectroscopic characterization, electrochemical behaviour, DNA binding, photonuclease activity and invitro antimicrobial efficacy", Spectrochimica Acta Part A: Molecular and Biomolecular Spectroscopy, 79: 873–883, (2011).

[13] Nagaveni, V.B., Mahadevan, K.M., Vijayakumar, G.R., Nagabhushana, H., Naveen, S., Lokanath, N.K., "Synthesis, crystal structure and excellent photoluminescence properties of copper (II) and cobalt (II) complexes with Bis(1[(4-butylphenyl)imino]methyl naphthalen-2-ol) Schiff base", Journal of Science: Advanced Materials and Devices, 3: 51–58, (2018).

[14] Zhang, J., Xu, L., Wong, W.Y., "Energy materials based on metal Schiff base complexes", Coordination Chemistry Reviews, 355: 180–198, (2018).

[15] Özkınalı, S., Gür, M., Şener, N., Alkın, S., Çavuş, M.S., "Synthesis of new azo schiff bases of pyrazole derivatives and their spectroscopic and theoretical investigations", Journal of Molecular Structure, 1174: 74–83, (2018).

[16] Anitha, C., Sheela, C.D., Tharmaraj, P., Sumathi, S., "Spectroscopic studies and biological evaluation of some transition metal complexes of azo Schiff-base ligand derived from (1-phenyl-2,3-dimethyl-4-aminopyrazol-5-one) and 5-((4-chlorophenyl)diazenyl)-2-hydroxybenzaldehyde", Spectrochimica Acta Part A: Molecular and Biomolecular Spectroscopy, 96: 493–500, (2012).

[17] Mallikarjuna, N.M., Keshavayya, J., Maliyappa, M.R., Shoukat Ali, R.A., Venkatesh, T., "Synthesis, characterization, thermal and biological evaluation of Cu(II), Co(II) and Ni(II) complexes of azo dye ligand containing sulfamethaxazole moiety", Journal of Molecular Structure, 1165: 28–36, (2018).

[18] Kakanejadifard, A., Azarbani, F., Zabardasti, A., Kakanejadifard, S., Ghasemian, M., Esna-ashari, F., Omidi, S., Shirali, S., Rafieefar, M., "The synthesis, structural characterization and antibacterial properties of some 2-((4-amino-1,2,5-oxadiazol-3-ylimino)methyl)-4-(phenyldiazenyl)phenol", Dyes and Pigments, 97: 215–221, (2013).

[19] Bal, S., Connolly, J.D., "Synthesis, characterization, thermal and catalytic properties of a novel carbazole derived azo ligand and its metal complexes", Arabian Journal of Chemistry, 10: 761–768, (2017).

[20] Slassi, S., Fix-Tailler, A., Larcher, G., Amine, A., El-Ghayoury, A., "Imidazole and azo-based Schiff bases ligands as highly active antifungal and antioxidant components", Heteroatom Chemistry, 2019: 6862170, (2019).

[21] Dutta, P., Mallick, D., Roy, S., Torres, E.L., Sinha, C., "Dihalo-bis[1-alkyl-2-{(o-thioalkyl)phenylazo}imidazole]zinc(II): structure, photochromism and DFT computation", Inorganica Chimica Acta, 423: 397–407, (2014).

[22] Khedr, A.M., Gaber, M., Issa, R.M., Erten, H., "Synthesis and spectral studies of 5-[3-(1,2,4-triazolyl-azo]-2,4-dihydroxybenzaldehyde (TA) and its Schiff bases with 1,3-diaminopropane (TAAP) and 1,6-diaminohexane (TAAH). Their analytical application for spectrophotometric microdetermination of cobalt(II). Application in some radiochemical studies", Dyes and Pigments, 67: 117–126, (2005).

[23] Pervaiz, M., Sadiq, S., Sadiq, A., Younas, U., Ashraf, A., Saeed, Z., Zuber, M., Adnan, A., "Azo-Schiff base derivatives of transition metal complexes as antimicrobial agents", Coordination Chemistry Reviews, 447: 214128, (2021).

[24] Venugopal, N., Krishnamurthy, G., Bhojyanaik, H.S., Giridhar, M., "Novel bioactive azo-azomethine based Cu(II), Co(II) and Ni(II) complexes, structural determination and biological activity", Journal of Molecular Structure, 1191: 85–94, (2019).

[25] Tawfik, A.M., El-ghamry, M.A., Abu-El-Wafa, S.M., Ahmed, N.M., "A new bioactive Schiff base ligands derived from propylazo-N-pyrimidin-2-yl-benzenesulfonamides Mn(II) and Cu(II) complexes: Synthesis, thermal and spectroscopic characterization biological studies and 3D modeling structures", Spectrochimica Acta Part A: Molecular and Biomolecular Spectroscopy, 97: 1172–1180, (2012).

[26] Anitha, C., Sheela, C.D., Tharmaraj, P., Johnson Raja, S., "Synthesis and characterization of VO(II), Co(II), Ni(II), Cu(II) and Zn(II) complexes of chromone based azo-linked Schiff base ligand", Spectrochimica Acta Part A: Molecular and Biomolecular Spectroscopy, 98: 35–42, (2012).

[27] Dinçalp, H., Yavuz, S., Haklı, Ö., Zafer, C., Özsoy, C., Durucasu, İ., İçli, S., "Optical and photovoltaic properties of salicylaldimine-based azo ligands", Journal of Photochemistry and Photobiology A: Chemistry, 210: 8–16, (2010).

[28] Mahmoodi, N.O., Nadamani, M.P., Behzadi, T., "New 1,3-diazabicyclo-[3.1.0]hex-3-ene photochromic azo dyes: Synthesis, characterization and spectroscopic studies", Journal of Molecular Liquids, 187: 43–48, (2013).

[29] Gilani, A.G., Taghvaei, V., Rufchahi, E.M., Mirzaei, M., "Tautomerism, solvatochromism, preferential solvation, and density functional study of some heteroarylazo dyes", Journal of Molecular Liquids, 273: 392–407, (2019).

[30] Ajaj, I., Assaleh, F.H., Markovski, J., Rancic, M., Brkovic, D., Milcic, M., Marinkovic, A.D., "Solvatochromism and azo–hydrazo tautomerism of novel arylazo pyridone dyes: Experimental and quantum chemical study", Arabian Journal of Chemistry, 12: 3463-3478, (2015).

[31] Sarigul, M., Kariper, S.E., Deveci, P., Atabey, H., Karakas, D., Kurtoglu, M., "Multi-properties of a new azo-Schiff base and its binuclear copper(II) chelate: Preparation, spectral characterization, electrochemical, potentiometric and modeling studies", Journal of Molecular Structure, 1149: 520–529, (2017).

[32] Dhaka, G., Kaur, N., Singh, J., "Spectral studies on benzimidazole-based ''bare-eye" probe for the detection of Ni^{2+}: Application as a solid state sensor", Inorganica Chimica Acta, 464: 18–22, (2017).

[33] Sondhi, S.M., Singh, N., Kumar, A., Lozach, O., Meijer, L., "Synthesis, anti-inflammatory, analgesic and kinase (CDK-1, CDK-5 and GSK-3) inhibition activity evaluation of benzimidazole/benzoxazole derivatives and some Schiff's bases", Bioorganic and Medicinal Chemistry, 14: 3758–3765, (2006).

[34] Mahmoodi, N.O., Rahimi, S., Nadamani, M.P., "Microwave-assisted synthesis and photochromic properties of new azo-imidazoles", Dyes and Pigments, 143: 387–392, (2017).

[35] Khungar, B., Rao, M.S., Pericherla, K., Nehra, P., Jain, N., Panwar, J., Kumar, A., "Synthesis, characterization and microbiocidal studies of novel ionic liquid tagged Schiff bases", Comptes Rendus Chimie, 15: 669-674, (2012).

[36] Kumaravel, G., Raman, N., "A treatise on benzimidazole based Schiff base metal(II) complexes accentuating their biological efficacy: Spectroscopic evaluation of DNA interactions, DNA cleavage and antimicrobial screening", Materials Science and Engineering: C, 70: 184–194, (2017).

[37] Wang, X., Xu, T., Duan, H., "Schiff base fluorescence probes for Cu^{2+} based on imidazole and benzimidazole", Sensors and Actuators B: Chemical, 214: 138–143, (2015).

[38] Özdemir, Ö., "Synthesis of novel azo linkage-based Schiff bases including anthranilic acid and hexanoic acid moieties: investigation of azo-hydrazone and phenol-keto tautomerism, solvatochromism, and ionochromism", Turkish Journal of Chemistry, 43: 266–285, (2019)

[39] Joseph, J., Suman, A., Nagashri, K., Joseyphus, R.S., Balakrishnan, N., "Synthesis, characterization and biological studies of copper(II) complexes with 2-aminobenzimidazole derivatives", Journal of Molecular Structure, 1137: 17–26, (2017).

[40] Kalarani, R., Sankarganesh, M., Vinoth, Kumar, G.G., Kalanithi, M., "Synthesis, spectral, DFT calculation, sensor, antimicrobial and DNA binding studies of Co(II), Cu(II) and Zn(II) metal complexes with 2-amino benzimidazole Schiff base", Journal of Molecular Structure, 1206: 127725, (2020).

[41] Zarei, S.A., "A mononuclear cobalt(II) salophen-type complex: Synthesis, theoretical and experimental electronic absorption and infrared spectra, crystal structure, and predicting of second- and third-order nonlinear optical properties", Spectrochimica Acta Part A: Molecular and Biomolecular Spectroscopy, 215: 225–232, (2019).

[42] Kumaravel, G., Utthra, P.P., Raman, N., "Exploiting the biological efficacy of benzimidazole based Schiff base complexes with L-Histidine as a co-ligand: Combined molecular docking, DNA interaction, antimicrobial and cytotoxic studies", Bioorganic Chemistry, 77: 269–279, (2018).

[43] El-wakiel, N., El-keiy, M., Gaber, M., "Synthesis, spectral, antitumor, antioxidant and antimicrobial studies on Cu(II), Ni(II) and Co(II) complexes of 4-[(1H-Benzoimidazol-2-ylimino)-methyl]-benzene-1,3-diol", Spectrochimica Acta Part A: Molecular and Biomolecular Spectroscopy, 147: 117–123, (2015).

[44] Almasi, M., Vilkova, M., Bednarcik, J., "Synthesis, characterization and spectral properties of novel azo-azomethine tetracarboxylic Schiff base ligand and its Co(II), Ni(II), Cu(II) and Pd(II) complexes", Inorganica Chimica Acta, 515: 120064, (2021).

[45] Horak, E., Kassal, P., Hranjec, M., Steinberg, I.M., "Benzimidazole functionalised Schiff bases: Novel pH sensitivefluorescence turn-on chromoionophores for ion-selective optodes", Sensors and Actuators B: Chemical, 258: 415–423, (2018).

[46] Chakraborty, S., Paul, S., Roy, P., Rayalu, S., "Detection of cyanide ion by chemosensing and fluorosensing technology", Inorganic Chemistry Communications, 128: 108562, (2021).

[47] Korolenko, S.E., Zhuravlev, K.P., Tsaryuk, V.I., Kubasov, A.S., Avdeeva, V.V., Malinina, E.A., Burlov, A.S., Divaeva, L.N., Zhizhin, K.Y., Kuznetsov, N.T., "Crystal structures, luminescence, and DFT study of mixed-ligand Zn(II) and Cd(II) complexes with phenyl-containing benzimidazole derivatives with linker C=N or N=N group", Journal of Luminescence, 237: 118156, (2021).

[48] Sıdır, Y.G., Sıdır, İ., Berber, H., Türkoğlu, G., "Solvatochromism and electronic structure of some symmetric Schiff base derivatives", Journal of Molecular Liquids, 204: 33–38, (2015).

[49] Tao, T., Xu, F., Chen, X.C., Liu, Q-Q., Huang, W., You, X-Z., "Comparisons between azo dyes and Schiff bases having the same benzothiazole/phenol skeleton: Syntheses, crystal structures and spectroscopic properties", Dyes and Pigments, 92: 916–922, (2012).

[50] Özdemir, Ö., "Synthesis of new luminescent bis-azo-linkage Schiff bases containing aminophenol and its derivative. Part I: Studying of their tautomeric, acidochromic, thermochromic, ionochromic, and photolüminesence properties", Journal of Photochemistry and Photobiology A: Chemistry, 380: 111868, (2019).

[51] Zhao, X.L., Geng, J., Qian, H.F., Huang, W., "pH-induced azo-keto and azo-enol tautomerism for 6-(3-methoxypropylamino)pyridin-2-one based thiophene azo dyes", Dyes and Pigments, 147: 318–326, (2017).

[52] Minkin, V.I., Tsukanov, A.V., Dubonosov, A.D., Bren, V.A., "Tautomeric Schiff bases: iono-, solvato-, thermo- and photochromism", Journal of Molecular Structure, 998: 179–191, (2011).

[53] Flores-Leonar, M., Esturau-Escofet, N., Mendez-Stivalet, J.M., Marin-Becerra, A., Amador-Bedolla, C., "Factors determining tautomeric equilibria in Schiff bases", Journal of Molecular Structure, 1006: 600–605, (2011).

[54] Bartyzel, A., Kaczor, A.A., "Synthesis, crystal structure, thermal, spectroscopic and theoretical studies of N_3O_2-donor Schiff base and its complex with Cu^{II} ions", Polyhedron, 139: 271–281, (2018).

[55] Orojloo, M., Amani, S., "Synthesis and studies of selective chemosensor for naked-eye detection of anions and cations based on a new Schiff-base derivative", Talanta, 159: 292–299, (2016).

[56] Tigineh, G.T., Liu, L.K., "Solvatochromic photoluminescence investigation of functional Schiff-bases: A systematic study of substituent effects", Journal of Photochemistry and Photobiology A: Chemistry, 338: 161–170, (2017).

[57] Joshi, H., Kamounah, F.S., Gooijer, C., van der Zwan, G., Antonov, L., "Excited state intramolecular proton transfer in some tautomeric azo dyes and Schiff bases containing an intramolecular hydrogen bond", Journal of Photochemistry and Photobiology A: Chemistry, 152: 183–191, (2002).

Fabricating of Turquoise/White Luminescent Azo-Schiff Bases Bearing Benzimidazole and Imidazole Rings

Özlem GÜNGÖR[1,*]

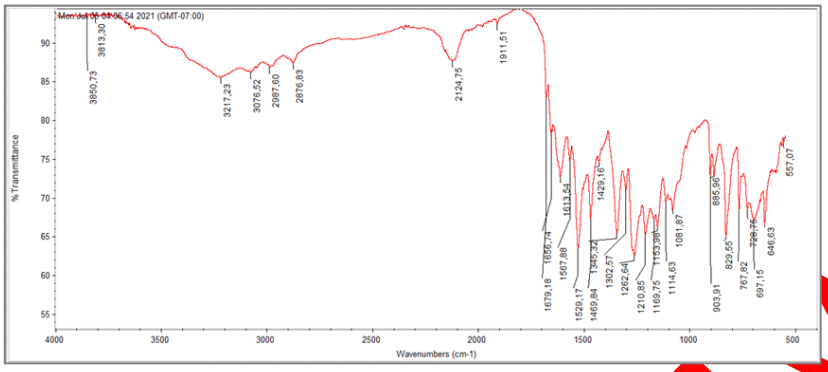

Figure S1**: FT–IR spectrum of **1a

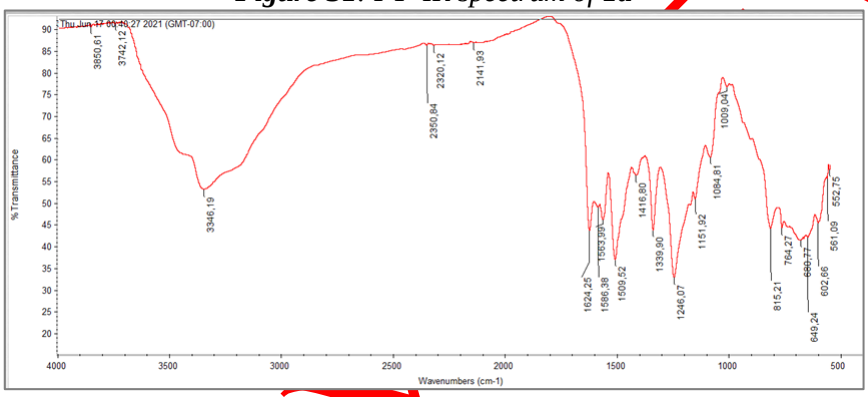

Figure S2**: FT–IR spectrum of **1b

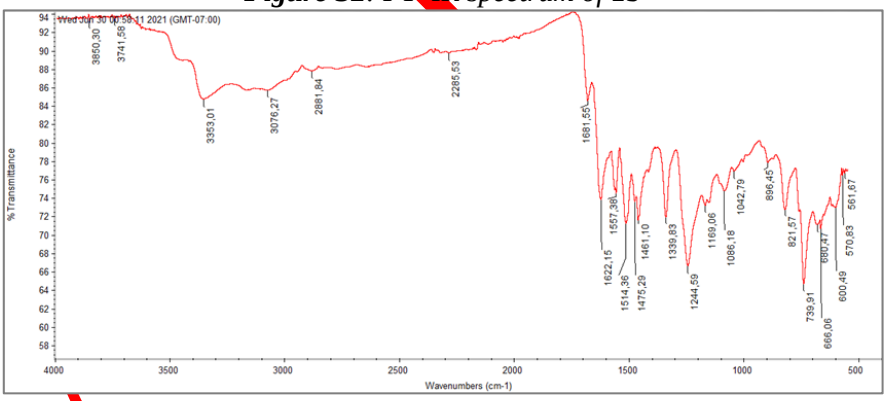

Figure S3**: FT–IR spectrum of **2a

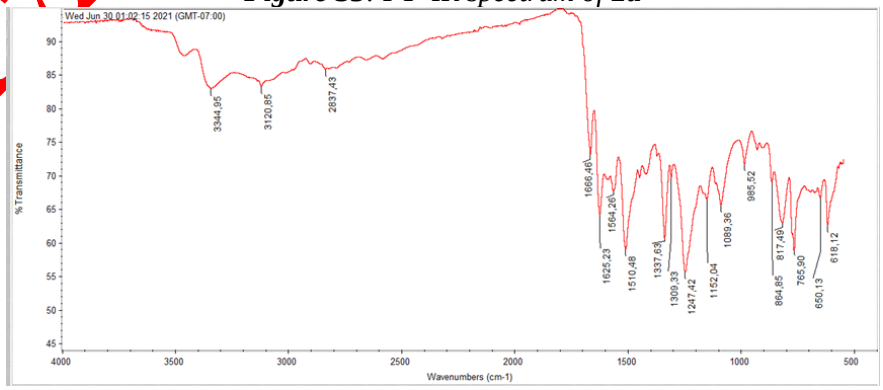

Figure S4**: FT–IR spectrum of **2b

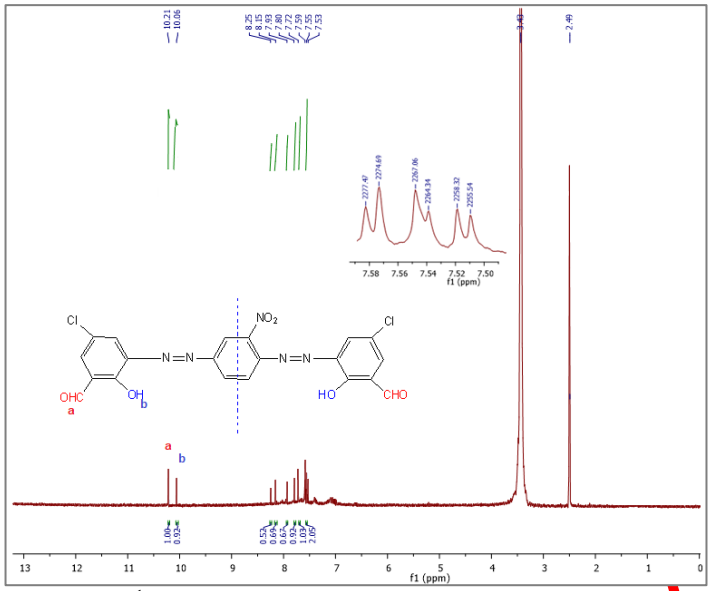

Figure S5. *^{1}H-NMR spectrum of **1a** in DMSO-d_6*

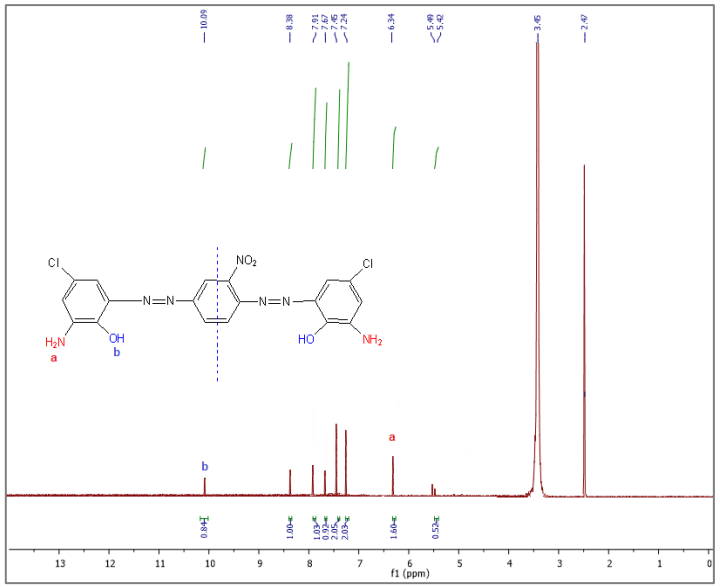

Figure S6. *^{1}H-NMR spectrum of **1b** in DMSO-d_6*

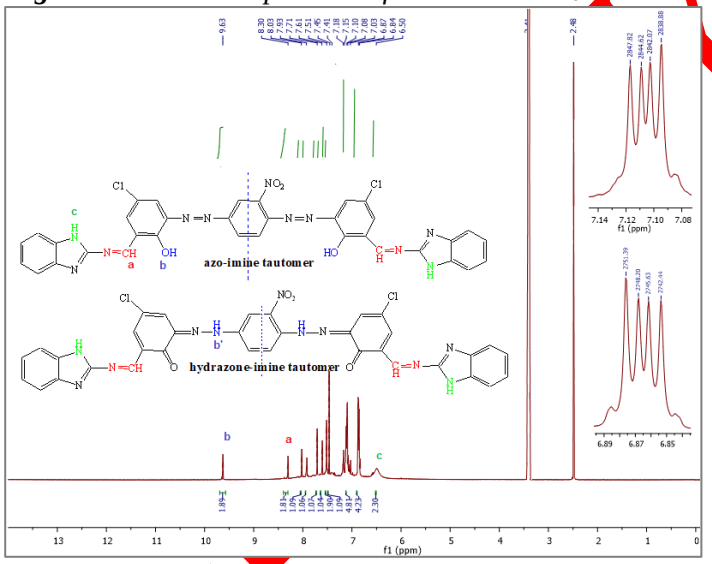

Figure S7. *^{1}H-NMR spectrum of **2a** in DMSO-d_6*

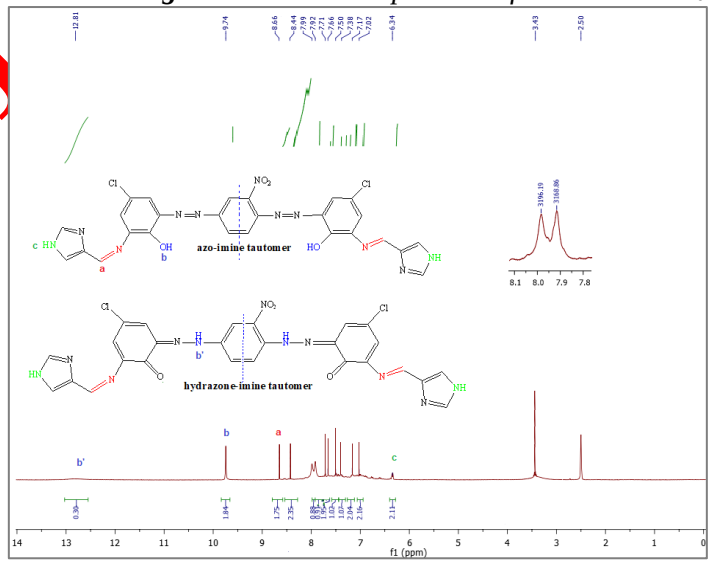

Figure S8. *^{1}H-NMR spectrum of **2b** in DMSO-d_6*

*e-mail: ozlemgungor@gazi.edu.tr

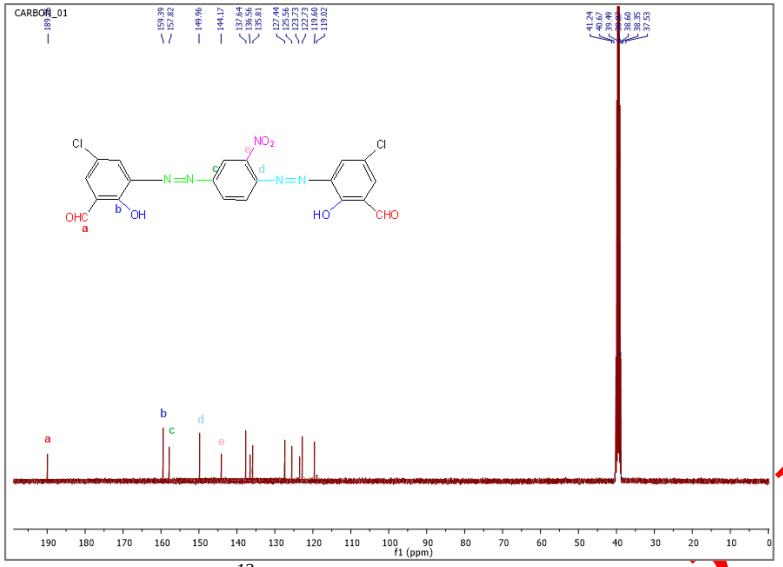

Figure S9. *^{13}C-NMR spectrum of* ***1a*** *in DMSO-d_6*

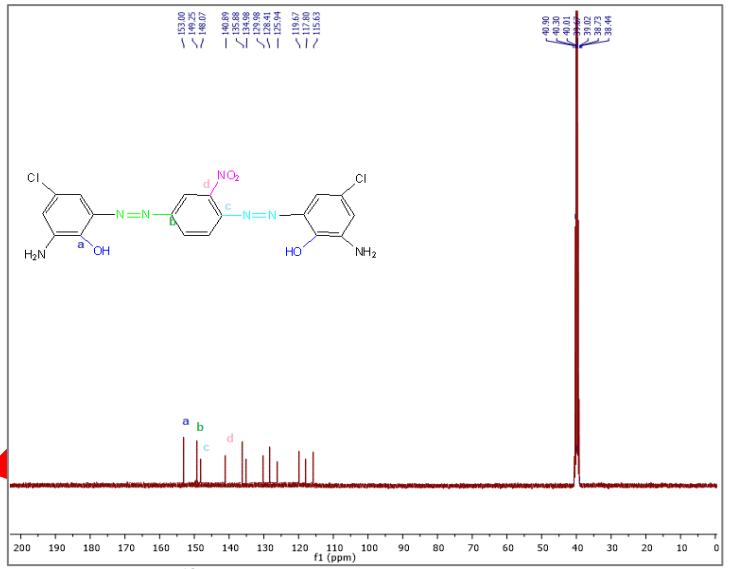

Figure S10. *^{13}C-NMR spectrum of* ***1b*** *in DMSO-d_6*

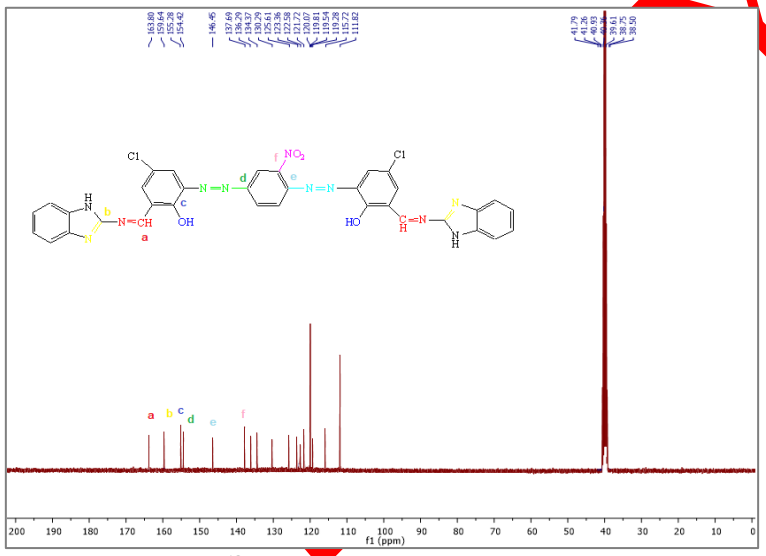

Figure S11. *^{13}C-NMR spectrum of* ***2a*** *in DMSO-d_6*

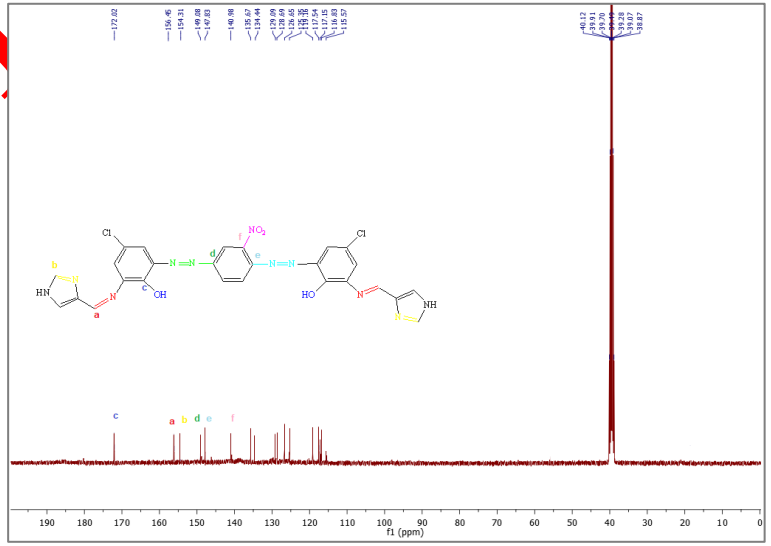

Figure S12. *^{13}C-NMR spectrum of* ***2b*** *in DMSO-d_6*

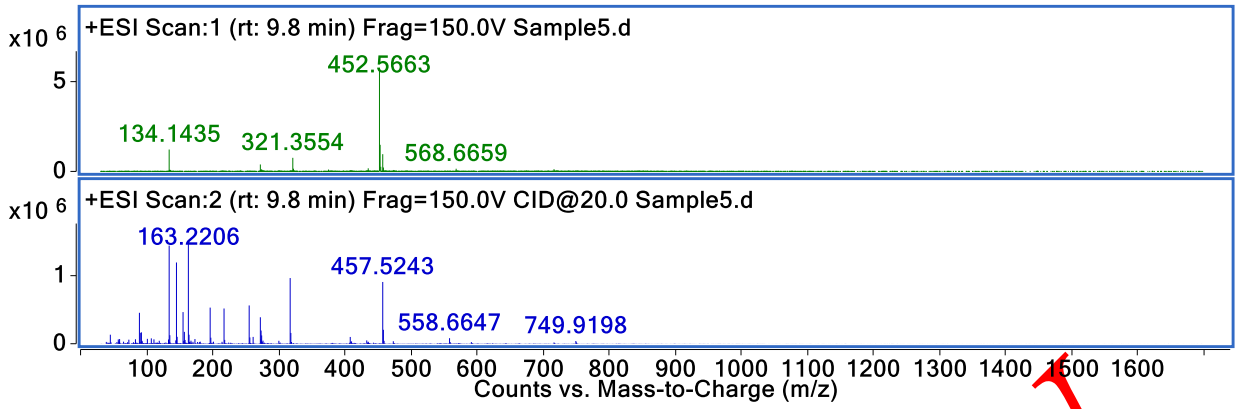

Figure S13. *Mass spectrum of* ***1a***

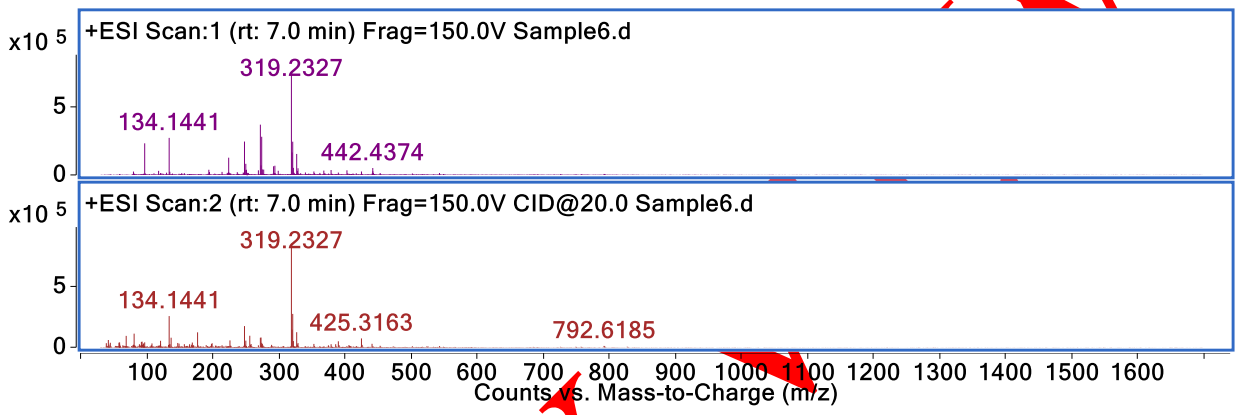

Figure S14. *Mass spectrum of* ***1b***

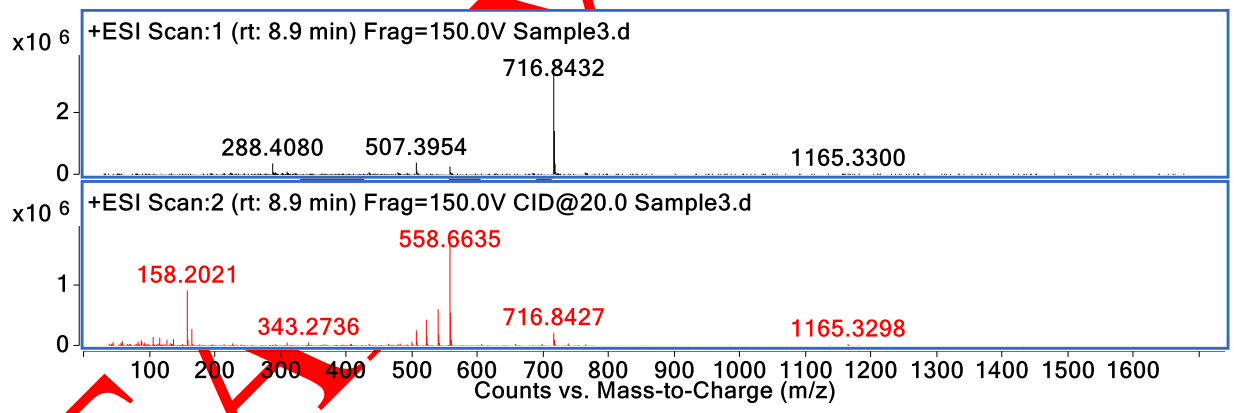

Figure S15. *Mass spectrum of* ***2a***

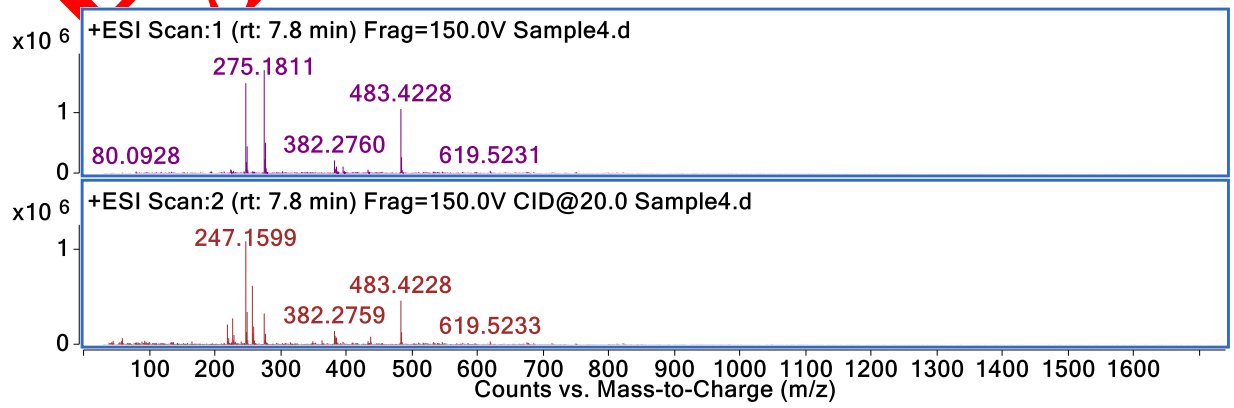

Figure S16. *Mass spectrum of* ***2b***

*e-mail: ozlemgungor@gazi.edu.tr

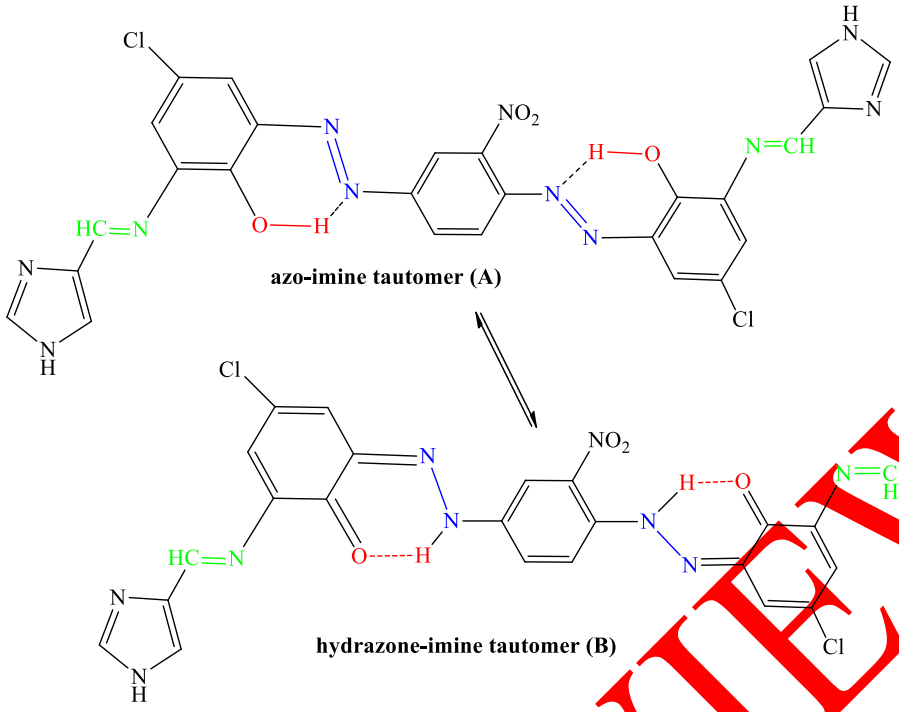

Figure S17. *Azo-hydrazone tautomeric equilibrium in* ***2b***

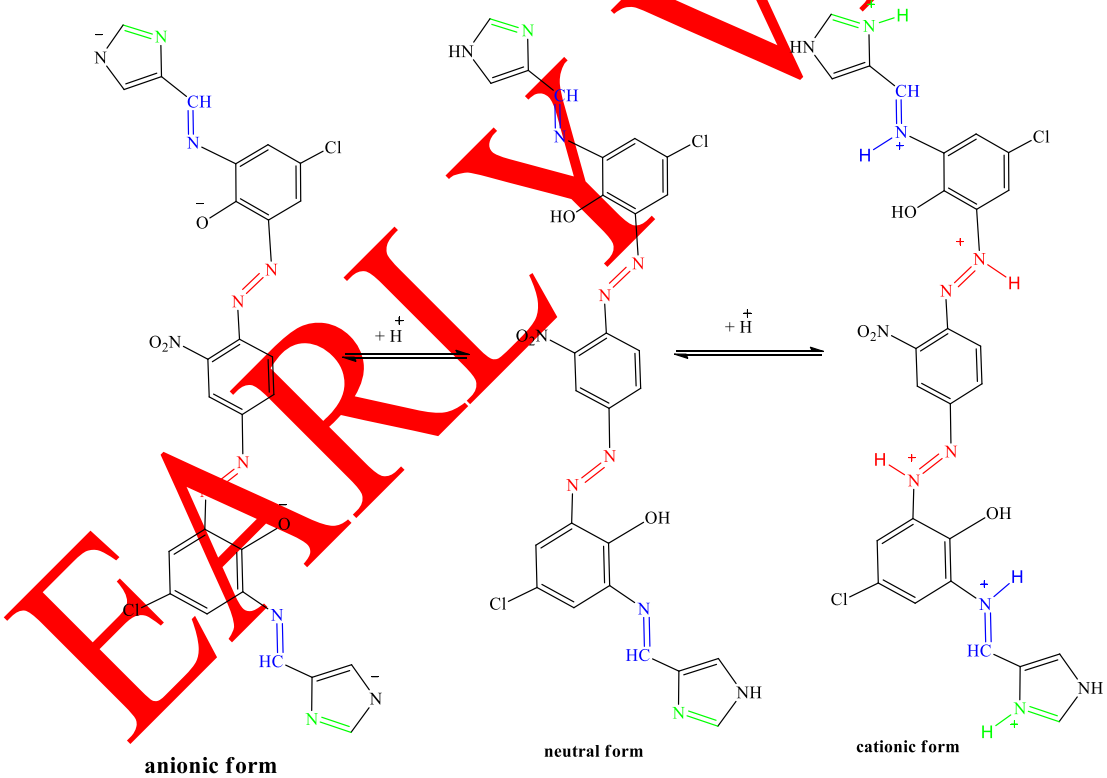

Figure S18. *Acid-base equilibrium in azo-imine tautomer of* ***2b***

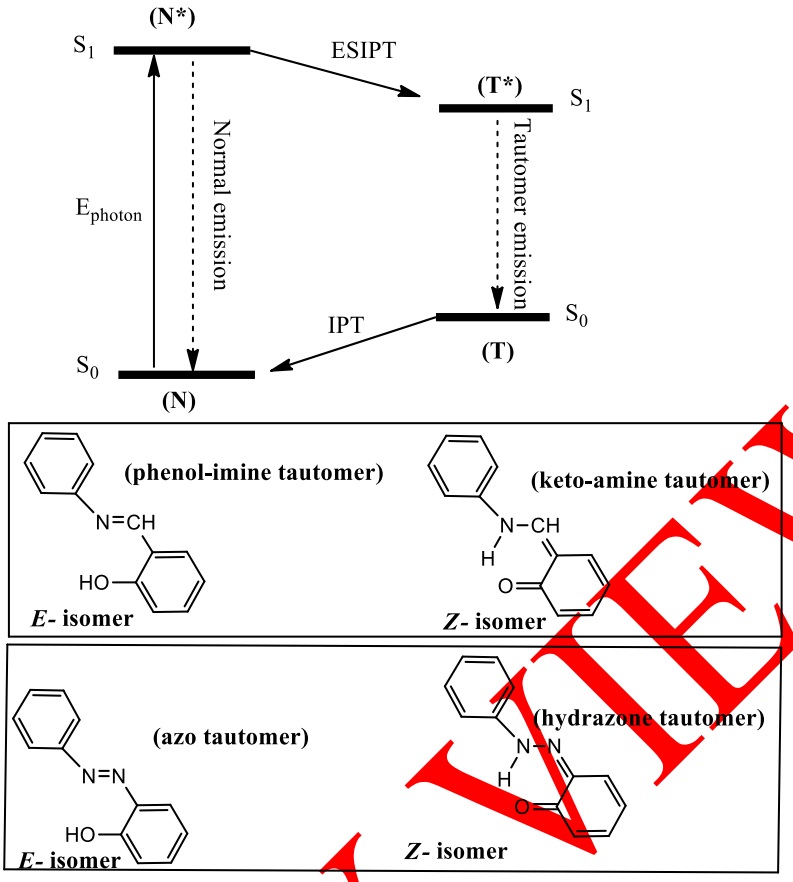

Figure S19. *General ESIPT reaction mechanism in Schiff bases and azo dyes*